Aus der Klinik für Urologie
der Medizinischen Fakultät Charité – Universitätsmedizin Berlin

DISSERTATION

Pharmacological reactivation of epigenetically regulated genes for identification of therapeutic targets and putative biomarkers in prostate cancer

zur Erlangung des akademischen Grades
Doctor medicinae (Dr. med.)

vorgelegt der Medizinischen Fakultät
Charité – Universitätsmedizin Berlin

von
Ikromov, Odiljon
aus Usbekistan

Datum der Promotion: 27.02.2015

This Dissertation was completed from October 2011-March 2014 at the Research Laboratory of Department of Urology of Charité-Universitätsmedizin Berlin under supervision PD Dr. med. Carsten Kempkensteffen.

Content

Zusammenfassung

Einleitung. Die Unterdrückung der Transkription von Tumorsuppressor-Genen durch aberrante Promotormethylierung spielt in der Entstehung diverser Tumorentitäten eine wichtige Rolle. Die vorliegende Arbeit beschreibt ein epigenetisches Screening-Verfahren zu Identifizierung bislang unbekannter Gene in Prostatakarzinomzellen, die durch diesen Mechanismus inaktiviert wurden.

Methoden. Re-exprimierte Gene in den Prostatakrebszelllinien LNCaP und DU-145 wurden nach der Behandlung mit dem DNA-Methyltransferase (DMNT) Inhibitor Zebularin analysiert.

Änderungen der Expressionsprofile zwischen behandelten und unbehandelten Zellen wurden zunächst mittels RNA-chip Technologie gemessen (Affymetrix Human Gene 1.0 ST). Für die Auswahl von geeigneten Genen, wurden bestimmte Kriterien wie das Vorhandensein von CpG-Inseln und SAGE-Datenbank-abgeleitete Expressionsdaten, definiert. Neun Kandidaten wurden mittels RT-qPCR in 50 gepaarten Proben von benignem Prostatagewebe und korrespondierendem Tumorgewebe aus Prostatektomiepräparaten, nach ihren erwarteten Expressionsmuster validiert.

Genexpressionsunterschiede zwischen benachbartem normalen und Tumorgewebe wurden statistisch ausgewertet (Wilcoxon-Test, Spearman Rangkorrelationskoeffizient). Die diagnostischen Variablen wurden durch Berechnung der Fläche unter der Kurve (AUC) quantifiziert.

Ergebnisse. Unser epigenetisches Screening-Verfahren entdeckte 51 Gene, die unseren Auswahlkriterien für eine methylierungsabhängige Regulation der Expression erfüllten. Vier von 8 Kandidaten, nämlich SARS, GADD45A, SPRY4 und ASNS waren im Karzinomgewebe erwartungsgemäß niedriger exprimiert als im korrespondierenden Normalgewebe. CTH, ABLIM3 und IFI6 waren hingegen nicht signifikant unterschiedlich exprimiert, und POTEF war im Tumorgewebe vergleichsweise überexprimiert. ROC-Analysen für SARS und GADD45A ergaben AUC-Werte von 0.816 bzw. 0.841 für die Unterscheidung von Tumor- und Normalgewebe. Weiterhin wurden positive Korrelationen der Expressionsniveaus zwischen diesen Genen gefunden.

Schlussfolgerung. SARS wurde erstmalig durch unsere Validierungsexperimente als differentiell reguliertes Gen im Tumorgewebe von Prostatakarzinompatienten beschrieben dessen Expression durch Promotor-Hypermethylierung gesteuert wird. Die verminderte Expression von SARS im

Tumorgewebe und seine physiologische Funktion deuten möglicherweise darauf hin, dass dieses Gen in die Tumorigenese des Prostatakarzinoms involviert ist. GADD45A und SPRY4, die bereits als hypermethyliert beim Prostatakrebs bekannt sind, wurden durch unsere Untersuchungen erwartungsgemäß als vermindert exprimierte Gene im Tumorgewebe bestätigt. Die Effektivität unseres experimentellen Ansatzes wird zusätzlich durch die Tatsache gestützt, dass das methylierungsabhängig regulierte GSTP1 in unseren Proben gleichfalls vermindert exprimiert war.

Abstract

Introduction. Transcriptional silencing associated with aberrant promoter hypermethylation is next to mutational changes a common mechanism of inactivation of tumor suppressor genes in cancer cells. The thesis describes an epigenetic screen aiming to discover hitherto unknown genes that are silenced by this mechanism in prostate cancer.

Method. Re-expressed genes were analyzed in the prostate cancer cell lines LNCaP and DU-145 after treatment with the DNA methyltransferase (DMNT) inhibitor zebularine.

Transcript expression changes in treated and untreated cells were compared using a whole genome expression microarray on Affymetrix Human Gene 1.0 ST. For candidate selection, we applied criteria like the presence of CpG islands and SAGE database-derived expression data. Next, we validated nine candidates for the expected expression pattern by RT-qPCR in 50 cases of paired normal and tumor tissue samples of prostate cancer patients who underwent radical prostatectomy.

Gene expression differences between adjacent normal and tumor tissues were statistically evaluated using two-tailed Wilcoxon test. Spearman's rank correlation was applied to calculate the relationship between expression levels of genes-of-interest coefficients. The performance of the diagnostic variables was quantified by calculating the area under the ROC curve (AUC).

Results. Our epigenetic screen revealed 51 genes that fitted our selection criteria for a methylation-dependent regulation. We found that 4 of 8 candidates: namely SARS, GADD45A, SPRY4, and ASNS are indeed downregulated in our prostate tumor tissues. CTH, ABLIM3, and IFI6 were not significantly regulated, and POTEF was significantly upregulated in tumor samples. In addition, ROC analyses showed 0.816 and 0.841 AUC curves in SARS and GADD45A, respectively. Also, positive correlations were found between these genes.

Conclusion. We found the gene SARS to be exclusively downregulated in our validation experiments in 50 paired prostate cancer specimens. This gene has not been described so far for its diminished expression in prostate cancer. This specific downregulation of SARS is most probably due to epigenetic downregulation by promoter hypermethylation. GADD45A, GSTP1 and SPRY4, reported to be

hypermethylated in prostate cancer by others, were downregulated in our sample set, too.

Abbreviations

AS	Active surveillance
AUC	Area under the curve
BPH	Benign prostatic hypertrophy
bp	Base pair
CpG	Cytosine and guanine linked by phosphate
Cq; Cp; Ct	Quantification cycle
cDNA	Complementary deoxyribonucleic acid
cRNA	Complementary ribonucleic acid
DNA	Deoxyribonucleic acid
DNMT	Deoxyribonucleic acid methyltransferase
DRE	Digital rectal examination
DSS	Disease-specific survival
E	Efficiency
fPSA	Free prostate specific antigen
mL	milliliter
mRNA	Messenger ribonucleic acid
µg	microgram
µL	microliter
ncRNA	Non-coding ribonucleic acid
nt	nucleotide
PCa	Prostate cancer
PCA3	Prostate cancer gene 3
PSA	Prostate specific antigen
RGE	Relative gene expression
RIN	Ribonucleic acid integrity number
RNA	Ribonucleic acid
ROC	Receiver operating characteristics
RT-qPCR	Real time quantitative polymerase chain reaction
SAGE	Serial analysis of gene expression
SARS	Seryl-tRNA synthetase
TNM	Tumor Node Metastasis
tPSA	Total prostate specific antigen
TRUS	Transrectal Ultrasonography
WW	Watchful waiting
XTT	2,3-bis-(2-methoxy-4-nitro-5-sulfophenyl)-2H-tetrazolium-5-carboxanilide
5-aza-CR	5-azacytidine
5-Aza-CdR	dihydro-5-azacytidine

Tables

Figures

1 Introduction

1.1 Prostate cancer epidemiology, diagnosis, staging, therapy, and prognosis

Prostate cancer (PCa) is the second most frequently diagnosed cancer and the fifth leading cause of cancer death among men worldwide, with 1,111,689 (15%) new cases and 307,471 (6.6%) deaths projected to occur in 2012 [1]. Three quarters of these cases and deaths are expected to occur in more developed countries [2]. PCa is the most common cancer in Germany and in the third position of cancer-specific causes of death after lung and colorectal cancer [3]. More than 68,000 (25.2%) cases, with a mortality rate of approximately 12,500 (10.7%) men, were newly diagnosed in 2008 [1].

PCa primarily affects elderly men at an average age of 65-69 years at first diagnosis. Age is the most prevalent risk factor and the age-specific mortality rates are increasing with age and the highest in the age group of ≥85 [2]. A positive family history increases the risk for PCa development. The risk is at least doubled when one first degree relative has PCa and the risk increases 5 to 11-fold when two or more first degree line relatives are affected by PCa [3, 4]. The incidence of clinical PCa prevalence differs widely between different geographical areas and remains at high levels in the USA and Northern Europe. Risk factors in PCa include diet, inflammation or sex hormone levels. For example, when Southeast Asian men move to the USA, their risk of PCa increases and may approach that of American men. However, the molecular circuits leading to PCa are similar in different ethnicities and equal access to urological services can result in equal outcomes [3, 5].

Digital rectal examination (DRE), serum concentration of prostate specific antigen (PSA), and transrectal ultrasonography (TRUS) are the main diagnostic tools that are used to diagnose PCa. The diagnosis is further verified by prostate needle biopsies or histopathological analysis of surgical specimens.

The DRE was the most widely used screening test for PCa until the introduction of PSA testing [6]. Most PCa (68%) that arise from the peripheral zone of the prostate may be detected by DRE. The other (24%) lesions develop in the transitional zone and central zone (8%) [7]. DRE is still an important diagnostic tool and continues to provide substantial prognostic information and should be performed together with PSA testing for early detection of PCa [6].

PSA (KLK3) is the most well-known member of the kallikrein-like serine protease family and certainly revolutionized the clinical practice for monitoring and detecting of PCa. It was discovered in the late 1970s and is synthesized almost exclusively by the

epithelial cells of the prostate [8, 9]. Although, PSA is organ-specific, it is not cancer-specific and displays a very low specificity for PCa diagnosis. The positive predictive value (PPV) is approximately 25%. Serum levels of PSA may be elevated due to different conditions such as: benign prostatic hyperplasia (BPH), prostatitis and other non-malignant conditions [9, 10]. A reliable discrimination between PCa and BPH is difficult, especially in patients with low PSA levels (2-10µg/l). Opportunities for a more reliable PSA diagnosis have increased using different forms of PSA such as: free PSA (fPSA), percent free PSA (%fPSA), [-2]-proPSA and PHI (prostate health index). These can help to avoid 20-25% unnecessary biopsies [9, 11, 12]. In addition, there are several helpful artificial neural network (ANN) tools to assess PCa risk and biopsy indication [13].

Recently, additional molecular markers like PCa gene 3 (PCA3, DD3) were introduced at least to support the clinical diagnosis and to reduce unnecessary biopsies. PCA3 is a PCa specific non-coding RNA (ncRNA), detectable in urine sediments after prostatic massage during DRE. It is strongly over expressed (around 60- to 100-fold) in more than 95% of prostate tumors when compared with benign prostatic tissue and it has shown its usefulness as a diagnostic tool. The main reason for using of the PCA3 urine test is to avoid a repeat biopsy [12, 14, 15]. Further markers, worth mentioning are certain types of gene fusions that connect the TMPRSS2 gene (transmembrane protease, serine 2) to members of the ERG/ETV family of genes (v-ets erythroblastosis virus E26 oncogene homolog (avian)). These markers significantly improve the ability to diagnose PCa [12, 16, 17].

Next to these “biochemical” markers, the histopathological assessment of prostate tissue is still the gold standard for reliable PCa diagnosis and therapy decisions. The need for prostate biopsies is determined according to clinical parameters such as PSA and a suspicious DRE. As already mentioned, an improved accuracy for biopsy indication can be achieved by measurements of %fPSA, [-2]-proPSA, and PCA3 [10, 11, 14, 16]. Core biopsies taken from different sites of the prostate and the Gleason score should be reported after histological examination. The Gleason grading is a unique system for assessing prostatic carcinoma. It is based on the sum of the most dominant primarily and secondary architectural (grade) patterns of the tumor (figure 1). Cells spread out and lose glandular architecture as the grade increases and tissue does not have recognizable (poorly differentiated) cells. This indicates the cancer

aggressiveness (figure 1). Consequently, cancers with a higher grade as the most dominant pattern are more aggressive and have a poor prognosis [18].

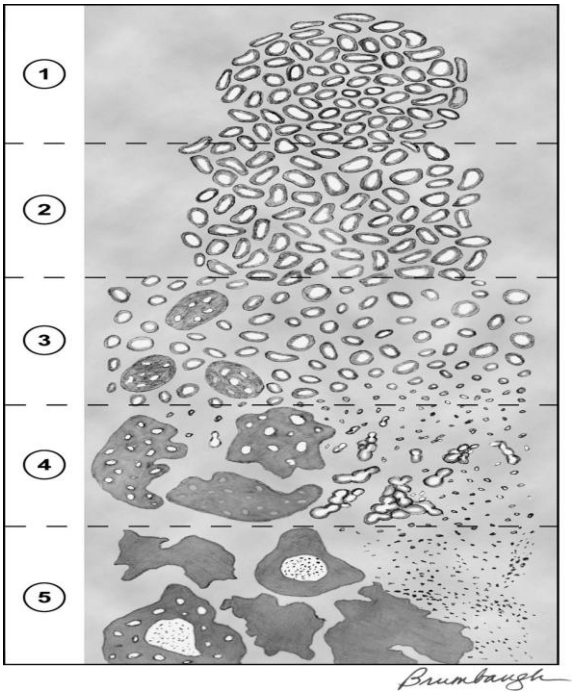

Figure 1. Histological diagram of Gleason score (Epstein et al., 2005) [18].

After radical prostatectomy, a tertiary pattern can be observed, apart from the primary and the secondary architectural patterns that has prognostic value [18].

Currently, the 7th edition of the Union Internationale Contre le Cancer (UICC) 2009 Tumor Node Metastasis (TNM) classification is used for staging of PCa. T describes the tumor size, invasion and extension (prostatic capsule, seminal vesicles, external sphincter, rectum and pelvic wall). T1 is clinically non-significant, T2 is organ-confined, a T3 tumor extends the prostatic capsule and infiltrates the seminal vesicles and the T4 tumor is attached to adjacent structures other than the seminal vesicles. N and M describe the processes of metastasis, the involvement of regional lymph nodes (N) and the occurrence of distant (M) metastases (bone, liver, and lung).

Watchful waiting, active surveillance, hormonal-, radio- or brachytherapy, and radical prostatectomy, are the therapy options for patients with different stages of PCa (EAU guidelines 2013).

PCa often grows very slowly. Watchful waiting (WW) was used to describe intensive type of follow-up in the pre-PSA screening era and not treat the less aggressive PCa in patients without progression of clinical symptoms. WW was usually

considered to be an option for elderly patients with significant comorbidity and for patients with limited life expectancy. In some WW studies, patients with T1-T2 Gleason ≤7, showed consistent 10 years disease-specific survival (DSS) ratio that ranged from 85 to 86.5% [19-21]. Active surveillance (AS) is the newly introduced term to describe the conservative management of PCa that helps to modify the therapy depending on change of tumor biology. Klotz et al.[22] reported AS cases with 99% DSS in 8 years' follow-up. Both methods aimed to reduce the ratio of overtreatment in patients with PCa [21, 22].

Radical prostatectomy (RP) is the surgical method of treatment that includes the removal of the entire prostate gland with seminal vesicles and sufficient surrounding tissue to achieve a negative margin. In some cases, the RP is followed by bilateral pelvic lymph node dissection (LND) [23]. Approximately 15 to 30% of patients do have a biochemical relapse after curative treatment with radical prostatectomy. Also, rates of incontinence and impotence after prostatectomy have varied from 5% to 65% and 29 to 100% of patients, respectively [19-24].

Transperineal brachytherapy is used less frequently due to the requirement of specially selected low-risk PCa patients. In patients with localized PCa (T1c-T2c N0 M0) and locally advanced PCa (T3-4, N0 M0), who decline surgical intervention, radiotherapy may be recommended (EAU guidelines 2013). Also, adjuvant radiotherapy is used in patients with positive margins and locally advanced PCa after RP that may be deferred until biochemical relapse is visible. Long-term androgen deprivation therapy (ADT) before and during radiotherapy is used to increase overall survival [25, 26]. Hormonal deprivation can be achieved either by orchiectomy (surgical castration) or by medical castration using LHRH analogues, steroidal and non-steroidal anti-androgens. In addition, new studies using novel drugs and drug combinations are in progress, which targeting cancer hallmarks, deliberately directed toward specific molecular targets [27]. Despite extensive scientific efforts and technological innovations in prostate carcinogenesis, the true reasons for development and progression to lethal PCa are still elusive and need further investigation.

1.2 Prostate cancer biology

PCa cells like any other cancer cells are characterized by various structural and functional changes when compared with their normal counterparts. Large-scale structural alterations on the DNA level (translocations, inversions and loss of

heterozygosity), small-scale structural alterations (insertions, duplications and deletions), and combinations of other genetic changes in cancer genes, together lead to the initiation, maintenance and progression of cancer. Approximately 400 somatically mutated cancer genes, comprising >2% of all known protein-coding genes in the human genome are known, and can be categorized into activated oncogenes and tumor suppressor genes (TSGs) [28].

Oncogenes altered by gain-of-function mutation, encode oncoproteins that stimulate cell growth and disrupt the normal cell cycle, which finally leads to cancer. The activation process may consist of gene amplifications (e.g.ERBB2 amplification in breast cancer), chromosomal translocations (e.g. MYC in B-cell lymphoma, TMPRSS2-ERG gene fusions in PCa), or point mutations (e.g. BRAF in melanoma).

TSGs protect cells from unrestrained growth. Inactivation of TSGs (that leads to loss of function) can be effected either by mutational rearrangements that disrupt the gene coding sequences (e.g. RB1 in retinoblastoma, p53 in many human cancers) or by epigenetic changes that do not alter the DNA sequence (e.g. p16 in colon or gastric cancer, VHL in renal cell carcinoma). Promoter hypermethylation and associated silencing of TSG transcription according to the Knudson two-hit hypothesis can constitute the first hit in somatic cancers and the second hit in the inherited tumors [29].

Inactivation of TSGs, as well as activation of oncogenes, give rise to tumorigenesis due to changes in the cellular physiology such as: abnormal growth signaling, resistance to apoptosis, avoidance of immune surveillance and reprogrammed energy metabolisms [27, 30].

All these genetic and epigenetic changes result in newly acquired functional characteristics of many different proteins that comprise the malignant phenotype and distinguish a cancer cell from a normal cell. These multistep biological changes in development of neoplastic diseases were reviewed by Hanahan & Weinberg [27]. The other cancer hallmarks include: evading growth suppressors, enabling replicative immortality, inducing angiogenesis and activation of invasion and metastasis. Recently, Hanahan & Weinberg further updated their review in the cancer hallmarks with the additional new emerging hallmarks mentioned above (deregulating cellular energetics and avoiding immune destruction) and two enabling characteristics (genome instability and mutation and tumor promoting inflammation) (figure 2) [27].

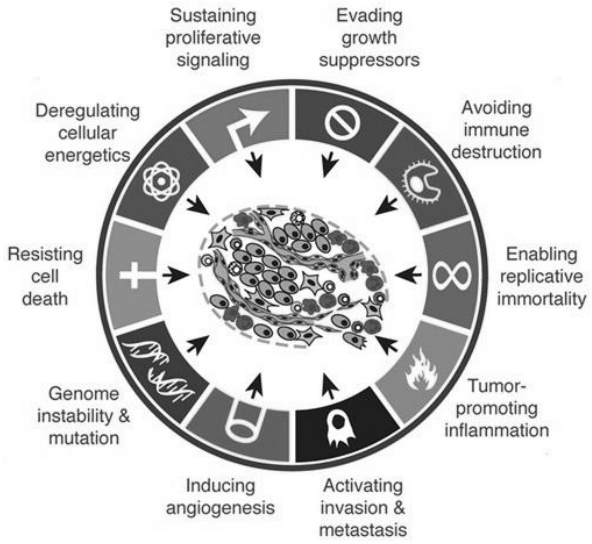

Figure 2. The hallmarks of cancer. This illustration encompasses the six originally proposed hallmark capabilities, and two emerging hallmarks (Deregulating cellular energetics and Avoiding immune destruction) and two enabling characteristics (Genome instability and mutation and Tumor promoting Inflammation) (Hanahan & Weinberg., 2011) [27].

1.2.1 Genetic alterations in prostate cancer

A recent survey of the PCa genome revealed a surprisingly low number of somatic mutations and other structural changes when compared with the genomes of other cancers [31]. This may reflect the relatively late onset of the carcinogenic process and favorable overall survival of most PCa cases. In addition to oncogene and TSG, current research based on complex analyses of entire cancer genomes by next generation sequencing (NGS) technologies, expression studies based on NGS-RNA sequencing (RNAseq) made it possible to distinguish between “driver” and “passenger” mutations. Although a specific assignment of distinctive drivers for certain cancers is still in its infancy [31, 32].

Genomic alterations in PCa most frequently occur on chromosome 8, including 8q gains with approximately 20-40% prevalence and 8p losses with approximately 30-50% prevalence. The oncogene MYC (8q24.1) and the tumor suppressor NKX3-1(8p21) are located on chromosome 8 [31, 33]. Other genomic alterations in PCa include the TMPRSS2-ERG gene fusion, deletion at 10q23.31 (PTEN) and at 17p31.1 (TP53), and focal deletions at 3p14.1-p13. The most commonly mutated gene is the androgen receptor (AR) [31].

MYC mRNA is elevated in most PCas and MYC may be a critical oncogenic event driving human PCa initiation and progression [34]. In comparison with MYC, NKX3-1 suppression plays an important role in initiation of PCa progression [35]. TMPRSS2 is more highly expressed in androgen-dependent PCas than in androgen-independent PCas. Fusion of androgen-responsive TMPRSS2 gene with ETS transcription factor family gene ERG is frequently overexpressed in PCa. Its presence in highly aggressive forms of PCa is associated with loss of function of tumor suppressor gene PTEN and these aberrations may be indicative of poor prognosis [36]. Progression of PCa and its resistance to ablation therapy is associated with loss of TP53, whereas rapidly developing PCa with metastases, and early death are associated with a loss of both PTEN and TP53 [37]. Apart from this, PTEN loss leads to suppression of NKX3-1[35].

1.2.2 Epigenetic alterations

The term epigenetics was introduced by Conrad Waddington in the 1950s [38]. Epigenetic changes have a recognized contribution to the carcinogenic process. The epigenetic alterations include histone modifications, non-coding RNAs, DNA methylation, and chromosomal remodeling [39].

These epigenetic changes are involved in the developmental process but are of exceptional interest for cancer biology, since they also provide a basis for genomic instability and may inhibit the expression of tumor suppressor genes. Epigenetic changes are a hallmark of human cancer and play a key role in the regulation of transcription, DNA repair, and replication processes. From a therapeutic viewpoint epigenetic changes (DNA methylation and histone acetylation) are of interest, since they are potentially reversible [27, 38, 39].

Histone modifications include histone methylation and acetylation. Methylation occurs in histone (H) side chains at arginine (R) and lysine (K) residues [40]. Mono-, di-, and trimethylation (me) by histone lysine methyltranferases (KMT) was observed in lysine, whereas arginine residues may be methylated symmetrically or asymmetrically [40, 41]. H3K4me2 and H3K4me3 levels were significantly increased in hormone-resistant PCa (HRPC) tissue, whereas the levels of H3K4me1, H3K9me2 and H3K9me3 were more reduced in cancer tissue than in non-cancerous tissue [42].

Except methylation, the N-terminal tail on the histone lysine residues may acetylate and deacetylate. Histone acetylation and deacetylation are regulated by the

histone lysine acetyltransferases (KATs) and the histone deacetylases (HDACs) enzymatic families [39, 40, 43]. Histone acetylation, as well as the other type of histone modifications, plays an important role in prostate carcinogenesis. Ellinger et al. reported reduced acetylation levels in H3 and H4 in PCa compared with nonmalignant tissue [42].

NcRNA is an RNA molecule that is not translated into protein and preserves epigenetic inheritance [39]. NcRNA genes include highly abundant and functionally important RNAs such as: transfer RNA (tRNA), ribosomal RNA (rRNA), small nucleolar RNAs (snoRNA), PIWI-interacting RNAs (piRNA), microRNAs (miRNA) and small interfering RNA (siRNA) family [40]. MiRNA expression profiles in human prostate tumors reveal a correlation not only with expression variations of protein-coding genes but also with clinic pathological parameters [39, 44]. MiR-101 was found to be silenced in PCa. It regulates the expression of EZH2 (enhancer of zeste homolog 2) that mediates neoplastic progression. EZH2 is the catalytic part of PRC2 (polycomb repressive complex 2) and participate in trimethylation of H3K27 [41, 45, 46].

DNA methylation is defined by heritable and congenital structural changes without altering the DNA sequence. DNA methylation occurs at the 5-carbon position of cytosine nucleotides (C) that precede a guanosine (G) in the DNA (i.e. CpG dinucleotides) leading to methylated cytosine residues (5mC). In normal cells, nearly all CpG dinucleotides in noncoding DNA are methylated and associated with the formation of inactive chromatin. This facilitates transcriptional silencing of noncoding regions and helps to inhibit illegitimate transcription of repeated elements of genome, inserted viral sequences and retrotransposons (figure 3) [29, 39, 47].

CpG dinucleotides are clustered in small stretches of DNA, thus forming a CpG-rich region or so called “CpG islands” [29]. CpG-rich regions of DNA are nonrandomly distributed and often surround the transcription start site. In cancer cells, CpG islands frequently become hypermethylated and thus cause the transcriptional silencing of their related genes (figure 3). The methylation of 5mC in CpG islands is the most widely studied epigenetic alteration and is in general associated with loss of gene function and transcriptional repression during cancer development. Under physiological conditions, methylated CpG islands are found in centromeres, telomeres, inactive X-chromosomes, and repeat sequences. [29, 40, 48, 49].

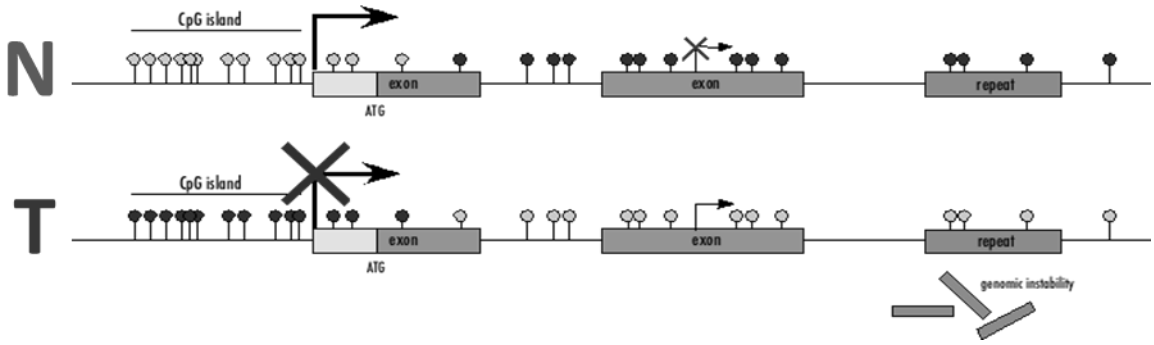

Figure 3. DNA methylation in normal and cancer cells. N- normal cells. T- tumor cells. White circles- normal CpG sites; black circles- methylated CpG sites.1, 2, 3- exons of the depicted gene. X- transcriptional repression. ATG- starting codon (Baylin 2005) [47].

Methylations of C residues are triggered by a family of enzymes called DNA methyltransferases (DNMTs). DNA methyltransferases 3 (DNMT3a and DNMT3b) act as de novo methyltranferases that establish DNA methylation during the embryogenesis, whereas DNA methyltransferase 1 (DNMT1) acts as the maintenance enzyme. DNMT1 identifies and methylates hemi-methylated DNA during DNA replication in S phase of the cell cycle. DNMT enzymes are active in normal as well as in cancer cells (figure 4) [40, 48, 50, 51].

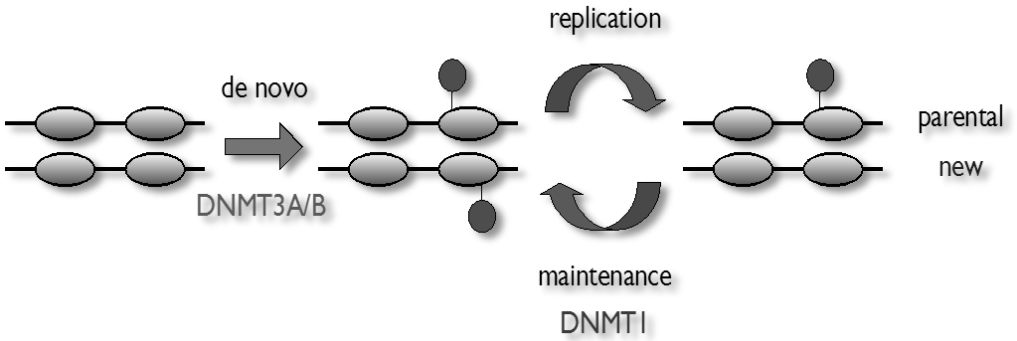

Figure 4. Congenital DNA hypermethylation and its maintenance. DNMT 1/3A/B- DNA methyltransferase (Grønbæk et al., 2007) [51].

Methylated cytosines may further be modified by hydroxylation to 5-hydroxymethylcytosine (5hmC) mediated by the ten-eleven translocations (TET1-3) family enzyme (figure 5). TET activity may further convert and form oxidative derivatives such as 5-formylcytosine (5fC) and 5-carboxylcytosine (5caC). Likewise, activation-induced deaminase (AID)/APOBEC-family of cytidine deaminase may deaminate 5mC

to thymine (T) (figure 5). So far, the biological function of these derivatives is not clear. They are believed to participate in the process of DNA methylation to increase the binding of some methyl-binding proteins (MBD) and have been identified in active and passive genes [40, 52, 53].

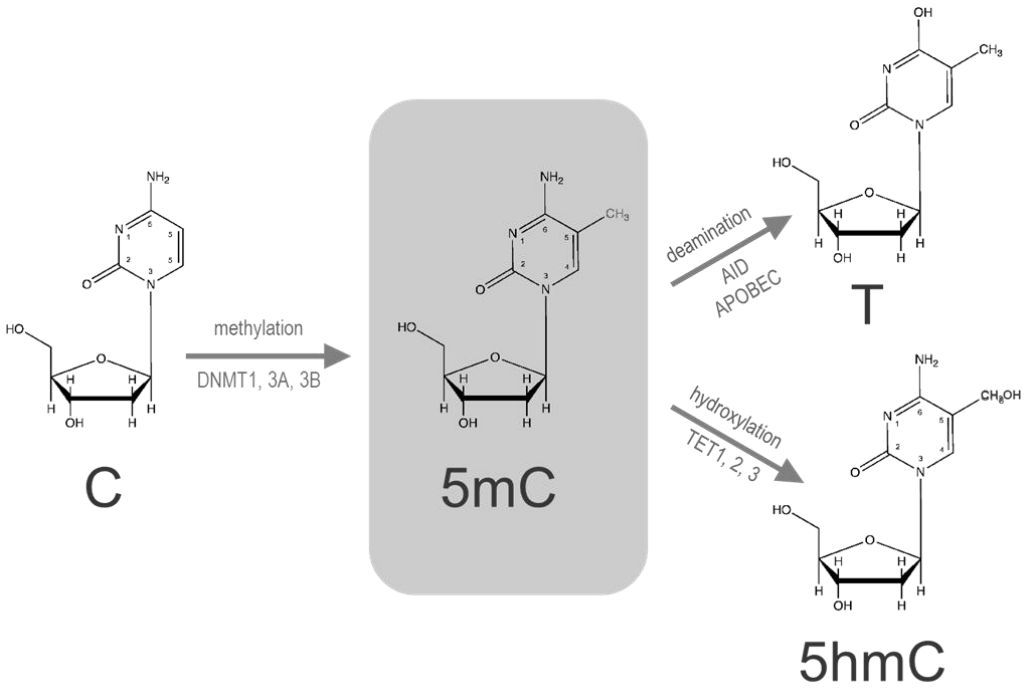

Figure 5. Cytosine modification pathways. The pathway includes cytosine methylation (5mC) by DNMTs, 5mC deamination (T) by AID/APOBEC and hydroxylation (5hmC) by TET1-3.

Methylation-specific PCR (MSP) is one the most common methylation detection tools. With this technique, totally methylated or totally unmethylated molecules are amplified, although the exact pattern of methylation is not reflected in the result [54]. New approaches, such as next generation whole genome bisulphite sequencing (WGBS) enable unbiased assessment of the entire DNA methylome. From a technological point of view, sodium bisulfite converts cytosine to uracil, which is converted into thymine during PCR amplification. Instead, 5mC residues are not converted and remain as cytosines. WGBS of treated DNA provide single nucleotide resolution of the methylation state of every cytosine and cover a whole genome (~95%) [49, 55].

An alternative indirect method to these rather expensive methods to detect methylation in general, individual genes silenced by methylation can be detected by

treatment of cells with DNMT inhibitors followed by expression analyses. Screening of differentially expressed genes of treated cells compared to untreated cells helps to reveal transcriptional upregulation of specific genes by demethylation. This “epigenetic screen” detects functionally relevant changes in methylation that might influence the tumorigenic processes [54].

A number of nucleoside DNMT inhibitors such as 5-azacytidine (5-Aza-CR), decitabine, dihydro-5-azacytidine (5-Aza-CdR), fazarabine, and zebularine have been known and widely used in clinical and laboratory experimental works [39, 56-59]. Well-known 5-Aza-CR and 5-Aza-CdR contain nitrogen in place of a carbon at position 5 of the pyrimidine ring (figure 6). Both of them have a strongly cytotoxic effect and are highly unstable in aqueous solutions. This limits their use in clinical practice. However, 5-Aza-CR and 5-Aza-CdR have been approved by the USA Food and Drug Administration (FDA) and are currently being used in hematology for the treatment of myelodysplastic syndrome. So far, there are no DNMT inhibitors that are used in solid tumors [56, 58].

Compared to the other demethylating agents of cytidine analog, zebularine is less toxic, stable in neutral solution, can be delivered orally and acts preferentially on cancer cells. Zebularine was originally developed as a cytidine deaminase inhibitor. It contains a 2-(1H)-pyrimidinone ring and lacks an amino group at position 4 of the pyrimidine ring (figure 6) [56, 60]. In this study, we used a moderate dose of zebularine to upregulate the silenced genes.

Figure 6. Chemical structures of cytidine, 5-azacytidine, and zebularine (www.biochemsoctrans.org).

There are many tumor suppressor genes in PCa known to be silenced due to promoter hypermethylation. Among them are GSTP1, APC, RASSF1, androgen (AR) and estrogen (ER-beta) receptor genes, cell-cell adhesion genes (CD44, CDH1), cell

cycle control genes (CCND2, CDKN1B, SFN) and apoptotic genes (PYCARD, RPRM, GLIPR1) [39, 49].

GSTP1 is the most promising biomarker candidate for PCa diagnosis, monitoring and prognosis [49, 61]. It has been first identified as being hypermethylated in PCa by Lee et al. in 1994 [62]. GSTP1 plays a key role in cellular detoxification of xenobiotics and carcinogenic agents, and acts as caretaker gene. Inactivation of GSTP1 makes cells sensitive to somatic alterations upon chronic exposure to genome-damaging stresses. Silencing of GSTP1 in PCa due to promoter hypermethylation is observed in >90% of tumors and in around 70% of high grade prostate interstitial neoplasia (PIN), but it is not detected in benign prostatic hyperplasia (BPH) [39, 49, 61, 62]. However, GSTP1 hypermethylation has been detected in several other cancer types, including breast and hepatocellular cancer [63, 64].

Besides DNA hypermethylation, DNA hypomethylation is found in certain types of cancer [39, 65, 66]. Schulz et al. reported that DNA hypomethylation might promote chromosomal instability, chromosome breaks, deletions, and amplification [65]. The genes WNT5A, S100P and CRIP1 are known to be activated in PCa due to promoter hypomethylation [66]. Multiple alterations on chromosome 8 that are believed to be important in the development and progression of prostate carcinoma, caused by genome-wide hypomethylation, were observed in the genes NKX3A and MYC [65].

1.3 Thesis aims

The objective of this research, using an epigenetic screen, is to discover genes that were hitherto unknown to be silenced by (promoter) hypermethylation in prostate cancer. Subsequently these genes were validated for expression differences in corresponding benign and malignant human tissue samples derived from radical prostatectomy specimen, to qualify them for their intended use as putative molecular markers for PCa.

For this purpose, the PCa cell lines LNCaP and DU-145 were treated with continuous doses of the DNMT inhibitor zebularine as a monotherapy. Appropriate isolation of cellular constituents after various treatments with the same regime and conditions were followed by state-of-the-art analytical measurements and statistical evaluations.

Special emphasis was put on selecting appropriate doses of zebularine for treatment. The efficacy of the treatment was checked by analyzing a set of genes

known to be downregulated by promoter hypermethylation. These genes were analyzed for their upregulation on the mRNA level (RT-qPCR).

Expression change of treated and untreated cells was compared using a whole genome expression microarray (Affymetrix). For candidate selection, we applied criteria that select for a methylation-based gene regulation (like the presence of CpG islands and SAGE database-derived expression data). Finally, “pre-selected” candidates were validated by RT-qPCR in adjacent normal and tumor tissue samples of PCa patients. Differences in gene expression were statistically evaluated.

2 Materials and methods

This chapter lists all equipment, reagents including commercially available kits, and essential methods to obtain the results that are presented in this dissertation.

2.1 Materials

2.1.1 Laboratory equipment

Instrument	Manufacturer
2100 Bioanalyzer	Agilent Technologies GmbH, Böblingen, Germany
Antares 48 Laminar Flow Box	Cotech Vertrieb GmbH, Berlin, Germany
Agagel Mini	Biometra, Goettingen, Germany
ARCR/UV work station	The CleanSpot. COY Laboratory Product, Michigan, USA
BioDoc CCD-Camera	BIOMETRA Biomedizinische Analytik GmbH, Göttingen, Germany
CB 210 Incubator	Binder, Tuttlingen. Germany
Coolpix 990	Nikon GmbH, Düsseldorf, Germany
Centrifuge 5415R	Eppendorf AG, Hamburg, Germany
Centrifuge 5430	Eppendorf AG, Hamburg, Germany
Centrifuge MiniSpin	Eppendorf AG, Hamburg, Germany
Centrifuge DW-41	QUALITRON, Inc., Korea
DM 2000 microscope	Leica Mikrosysteme Vertrieb GmbH, Wetzlar, Germany
Gen Amp PCR system 9700	Applied Biosystems, Norwalk, Germany
Gradient Cycler	BIO-RAD, USA
HT III photometer	Anthos Labtech Instruments GmbH, Wals-Siezenheim, Austria
Horizon 11-14 Horizontal Gel Electrophoresis	LIFE TECHNOLOGIES, Gaithersburg, MD, USA
JUNG FRIGOCUT 2800E	Leica Instrument GmbH, Nussloch, Germany
Leitz DMRBE fluorescence microscope	Leica Mikrosysteme Vertrieb GmbH, Wetzlar, Germany
Leitz Fuovert Microscope	Leica Mikrosysteme Vertrieb GmbH, Wetzlar, Germany
LightCycler 480	Roche Applied Sciences, Mannheim, Germany
NanoDrop ND-1000	Thermo scientific, Wilmington, DE, USA
Power PAC 3000	BIO-RAD, USA
Thermomixer 5436	Eppendorf AG, Hamburg, Germany
Vortex VF2	Kanke&Kunkel KIKA Labortechnik

2.1.2 Consumables

Consumables	Manufacturer
Falcon cell cultureware (T25 flask, 96 well plate)	BD Biosystems, Heidelberg, Germany
Primaria cell cultureware (T25 flask, 96 well plate)	BD Biosystems, Heidelberg, Germany
White 96-well RT-qPCR plates Cat. No.04729692001	Roche Applied Sciences, Mannheim, Germany

2.1.3 Cell lines, chemicals, reagents and kits

Cell line	Manufacturer
DU-145 cell line	American Type Culture Collection (ATCC) (ATCC® Number: HTB-81™)
LNCaP cell line	American Type Culture Collection (ATCC) (ATCC® Number**:** CRL-1740™)
Kit for cell line	**Manufacturer**
Cell Proliferation Kit II (XTT) (Cat. No.11465015001)	Roche Applied Sciences, Mannheim, Germany
Growth media for DU-145 and LNCaP cell line	**Manufacturer**
500 mL RPMI 1640	Invitrogen, Darmstadt, Germany
10% FCS	PAA, Pasching, Austria
1 x Penicillin/Streptomycin	PAA, Pasching, Austria
Staining solution	**Manufacturer**
100µg/mL Acridine orange	Sigma Aldrich, München, Germany
100µg/mL Ethidium bromide	Sigma Aldrich, München, Germany
100 mL pH 7.2 Dulbecco's PBS	PAA, Pasching, Austria
Other chemicals and reagents	**Manufacturer**
Trypan Blue 0.2%	Waldeck GmbH und Co. Kg., Münster, Germany
zebularine	SIGMA, USA
Dulbecco's PBS	PAA, Pasching, Austria
DMSO	Sigma Aldrich, München, Germany

2.1.4 RNA isolation, cDNA Synthesis, PCR, and agarose gel electrophoresis

RNA extraction and cDNA Synthesis	Manufacturer
Agilent RNA Nano kit 6000 (Cat. No.5067-1511)	Agilent technologies, Waldbronn, Germany
miRNAeasy Mini Kit (Cat. No.217004)	Qiagen, Hilden, Germany

Transcriptor First Strand cDNA Synthesis (Cat. No.04896866001)	Roche Diagnostics, Mannheim, Germany
Chloroform	Sigma Aldrich, München, Germany
Ethanol, absolute	J.T. Baker, Deventer, Holland
PCR	**Manufacturer**
LightCycler480 Probes Master (Cat. No.04707494001)	Roche Diagnostics, Mannheim, Germany
Amplification primers	TIB MOLBIOL, Berlin, Germany
Probes (Universal Probe library)	Roche Diagnostics, Mannheim, Germany
Ready to use HPRT1 (Cat.No.05046157001)	Roche Diagnostics, Mannheim, Germany
Ready to use TBP (Cat.No.05189284001)	Roche Diagnostics, Mannheim, Germany
Ready to use PBGD (Cat.No.05046149001)	Roche Diagnostics, Mannheim, Germany
AmpliTaq Gold Polymerase	Invitrogen, Darmstadt, Germany
Agarose gel	**Manufacturer**
0.25% Bromo phenolblue	Sigma Aldrich, München, Germany
50X TAE electrophoresis buffer	Thermo SCIENTIFIC, Vilnius, Lithuania
Agarose Electrophoresis grade	Invitrogen, UK
100bp DNA Ladder	Invitrogen, UK

2.1.5 Software

Software	Manufacturer	Main usage
FileMaker Pro 10.0v1	FileMaker, Inc., CA, USA	Patients data record
Oligo 6	Molecular Biology Insights, Inc. CO, USA	Primer design
EMBOSS-CpG blot	European Bioinformatics Institute, Cambridge, UK	CpG island identification
Digital Northern	National Cancer Institute, Maryland, USA	in silico gene expression data
GenEx Professional 4.3.7	MultiD Analyses AB, Sweden	RT-qPCR
qBase^{PLUS}	Biogazelle, Zwijnaarde, Belgium	Reference gene selection
GraphPadPrism® 5	GraphPad Software, Inc., La Jolla CA, USA	Statistical analyses
MedCalc 9	MedCalc Software, Mariakerke, Belgium	Statistical analyses
IBM® SPSS® Statistics 19	SPSS, Inc., an IBM Company, USA	Statistical analyses
Pubmed	NCBI, Maryland, USA	Literature and gene research

GeneCard® The Human gene compendium	Weizmann Institute of Science, Gene research Rehovot, Israel

2.2 Experimental methods

2.2.1 Tissue sample collection, histopathology, and RNA isolation

Tissue samples were collected from patients undergoing radical prostatectomy (RPx) between 2002 and 2004 at the Charité – Universitätsmedizin Berlin, Campus Benjamin Franklin, Berlin, Germany. All patients were informed and agreed before the operation for anonymous material transfer for research purposes. The study was done according to the regulations of the ethics board of the university. For this study, 50 cases were chosen based on the sole criteria of a high percentage of tumor content in their analyzed tissue samples (see below). Clinical data (follow up time after surgery and PSA data), and histopathological data (grade, UICC 2002 TNM stage, Gleason grading etc.) were obtained for each individual case and stored anonymously in a local FileMaker database.

Fresh prostate tissue was obtained under supervision of an uropathologist 15-30 min after surgery. Sliced tissue samples were snap-frozen in liquid nitrogen and later stored at -80°C for further analysis. Histological evaluation of these samples was performed by an external uropathologist (PD Dr. med. Jens Köllermann). The samples were stained with hematoxylin–eosin (H/E) to verify tumor content and to distinguish areas of nonmalignant and malignant tissue. Stained samples were analyzed for their Gleason pattern and grouped according to their tumor content. Only samples containing >60% of tumor cells were used for further investigation.

For tissue RNA isolation frozen, blocks marked by the pathologist were mounted at -25ºC and serially sectioned in the “JUNG FRIGOCUT 2800E” instrument. Details of the RNA isolation method are described in chapter 2.2.5.

2.2.2 Prostate cancer cells treatment

For treatment of PCa cells, as models of demethylation-induced transcriptional upregulation, we used the androgen sensitive cell line LNCaP (ATCC® Number: CRL-1740™) and androgen insensitive DU-145 cells (ATCC® Number: HTB-81™). The identity of our PCa cell lines was verified by the German Prostate Cancer Consortium in 2009 (Prof. G. Unteregger, University Homburg, personal communication). The cells were cultured in T25 flasks filled with 5mL RPMI medium supplemented with 10% FCS,

100U/mL penicillin and 100µg/mL streptomycin. The flasks were incubated at 37°C and 5% CO_2 in a humidified atmosphere. PCa cells were grown to a density of 70 to 90% and seeded into appropriate tissue culture plates. Once the cells reached confluence, they were detached from the surface by treatment with the trypsin/EDTA solution. The DNA methyltransferase (DNMT) inhibiting reagent zebularine SIGMA was used as a 20mmol/L stock solution dissolved in PBS and stored in aliquots at -20°C. Except for specific experiments (see below), the cells were treated with a final concentration of 100µM zebularine. Treatment usually started 24 hours after seeding. Growth medium containing zebularine was replaced after 2-3 days. Cells were split at least once during the treatment period. Three experiments with the same treatment protocol were performed subsequently. A general outline of the treatment regime is shown in figure 7. For further experimental evaluation, cells were harvested as PBS-washed (2x) pellets, snap-frozen in liquid nitrogen and kept at -80ºC.

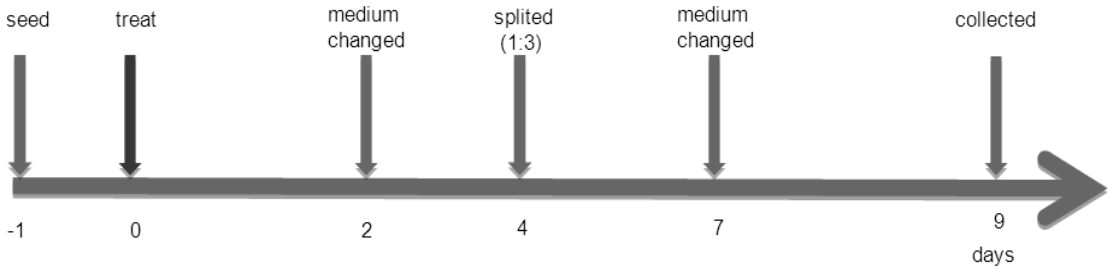

Figure 7. General outline of treatment of PCa cell line Du-145 and LNCaP.

2.2.3 XTT cell proliferation assay

Cell proliferation and toxicity of the zebularine was assessed with the XTT-Test (Roche). This method is based on the ability of the vital cells to convert the yellow tetrazolium salt (2,3-bis-(2-methoxy-4-nitro-5-sulfophenyl)-2H-tetrazolium-5-carboxanilide) to orange formazan. The intensity of this water-soluble dye is proportional to the number of metabolically active cells.

For this purpose, cells are grown in flat-bottom 96 well plates at cell concentrations ranging from 3000 cells/well for DU-145 to 6000 cells/well for LNCaP. After 1 day, the cells were treated with zebularine at concentrations of 100µM for a proliferation time ranging from 48 to 96 hours. At the end of each experiment XTT, labeling mixture (1 part activation solution: 50 parts XTT reagent) was added to the cells

for 4 hours at same temperature. Formazan dye absorbance intensity was measured with the Anthos HTIII multi-well spectrophotometer reader at a wave-length of 475nm.

2.2.4 Morphological assessment of apoptosis by fluorescent microscopy

To provide further evidence on the low to moderate cytotoxicity of the zebularine treatment, we used a quick and easy to handle assay that is based on the determination of plasma membrane integrity in live and dead cells. Acridine orange crosses the cell membrane of a vital cell to allow it to incorporate into the DNA of the cells and to stain them green. Cells with damaged membranes (apoptosis and/or necrosis) are additionally permeable to ethidium bromide that does not enter living cells. In the case of damaged cells, both dyes intercalate into DNA. These cells then turn orange, since the orange fluorescence of ethidium bromide is added to acridine orange green color.

DU-145 and LNCaP were cultured in flasks specifically designed for microscopic analysis and treated with different concentrations of zebularine (0, 100µM, 200µM) for 48 to 96 hours. The culture medium was replaced with PBS containing an acridine orange/ethidium bromide mixture (prepared 1:1, each 100µg/mL final concentration) and incubated for two minutes. The coverslips with stained cells were mounted and examined under fluorescent microscope (Leica DMRBE microscope). Cell viability was visually calculated as percentage of green cells (living cells) from the total number of cells seen in each chamber area.

2.2.5 RNA isolation and quality control

Total RNA was extracted from treated and mock PCa cells (LNCaP and DU-145) with the miRNeasy Mini Kit Qiagen. The same kit was used to isolate RNA from fresh frozen PCa adjacent normal and tumor tissues (see, chapter 2.2.1 above). Approximately 1 x 10^6 harvested cells were lysed in 700µL QIAzol lysis reagents. Tissue cores were sliced into multiple thin pieces (approximately 20mg) and homogenized also in 700µL QIAzol lysis reagent. After centrifugation at 4°C for 15min at 12000g, upper aqueous RNA partition was purified using a spin-column according to the manufacturer's protocols. RNA was eluted into 40µL H_2O.

RNA concentration and purity was determined spectrophotometrically on a Nanodrop ND-1000 instrument. All RNA samples were free from remaining proteins (260/280nm ratio ~1.8 to 2.0) and other contaminations (260/230nm ratio = 2.0 to 2.2). Samples with ratios below 1.8 were excluded from subsequent analysis. In addition, RNA integrity was assessed by capillary electrophoresis on the Bioanalyzer-2100. Only

RNA samples form cell lines with RIN numbers above 8 were used for RNA chip analysis. Likewise, only tissue RNA samples with RIN ≥5.7 were used for further investigation of tissue RNA. The extracted RNA was stored at -80°C.

2.2.6 Microarray analysis

RNA microarray is a powerful technology for biological or medical investigations that allows the expression status of entire transcriptomes to be simultaneously measured and compared. Microarray GeneChip® analysis was performed at the “Labor für Funktionelle Genomforschung” (LFGC, Dr. U. Ungethüm), a core facility of the Charité – Universitätsmedizin Berlin. Total RNA extracted from treated and untreated PCa cell lines DU-145 and LNCaP was analyzed using Human Gene 1.0 ST arrays. This chip covers 36079 probes that represent 21014 genes. For our data collection, we used 12 arrays to analyze the transcriptome of three independent experiments in both cell lines.

Standard protocols were used by the LFGC for the first and second cycle cDNA synthesis. 300ng of total RNA was used for cDNA synthesis. During the following “*in vitro”* transcription reaction, cRNA was obtained and used as starting material for the second cycle cDNA synthesis.

Background adjustment, normalization, pre-processing of these arrays to combine the probe pair intensities and principal component analyses (PCA) were also performed at the LFGC.

The raw data were normalized according to the log scale robust multi-array analysis (RMA). Briefly, signal intensities were background-adjusted to obtain perfect match (PM) intensities and a quantile normalization approach was performed across all arrays of the experiment. In order to control the false discovery rate at $\alpha<0.05$ for array data, we applied the false discovery rate multiple testing correction according to Benjamini and Hochberg [67].

Mean of fold changes were calculated and data were condensed.

All RNA chip data have been deposited in the National Center for Biotechnology Information GEO database under the access No. GSE51629 (http://www.ncbi.nlm.nih.gov/geo/query/acc.cgi?acc=GSE51629).

2.2.7 cDNA synthesis

Total RNA from PCa cell culture (DU-145, LNCaP) and adjacent normal and tumor tissue, was reverse transcribed using the reagents of the “Transcriptor First-Strand cDNA Synthesis Kit” (Roche). 1µg of total RNA was reverse transcribed using a combination of anchored-oligo (dT) priming and random hexamer priming. cDNA synthesis was performed according to the manufacturer’s instructions. The synthesized cDNAs was stored at -20°C. The cDNA synthesis and cycling protocols are outlined in tables 1 and 2 below.

Table 1. cDNA synthesis

Components	Volume	Concentration
Total RNA	10µL	1µg
Anchored-oligo (dT) primer	1µL	2.5µM
Random hexamer primer	2µL	60µM
cDNA synthesis mix	Volume	Concentration
Transcriptor Reverse Transcriptase Reaction Buffer	4µL (1×) (8mM MgCl2)	
Protector RNase Inhibitor	0.5µL	20U
Deoxynucleotide Mix,10 mM	2µL	1mM
Transcriptor Reverse Transcriptase	0.5µL	10U
Total	20µL	

Table 2. Reverse transcription

	Preparation	
Steps	Time	Temperature
Denaturation	15 min	65°C
	∞	4°C
	cDNA synthesis	
Annealing	10 min	25°C
Elongation	30 min	55°C
Inactivation	5 min	85°C
	∞	4°C

2.2.8 Amplification of cDNAs

To check if the cDNA synthesis was successful, we used a PCR protocol for the commonly used reference gene PGBD in combination with primers synthesized by TIB MOLBIOL. The primer sequences are as follows: PBGD forward 5'-TGCAACGGCGGAAGAAAAC-3'; PBGD reverse 5'- GGCTCCGATGGTGAAGCC-3'. Reaction components and cycling conditions are given in tables 3 and 4.

PCR products of gene PBGD were separated on agarose gels to confirm the specificity and consistency of cDNA synthesis reaction. The expected size of the product was 313bp (figures 8 and 9). Fragments were separated at a constant voltage of 100V for 70 min. Each gel was analyzed and exposed for 30 seconds on the BioDoc-Camera (BIOMETRA).

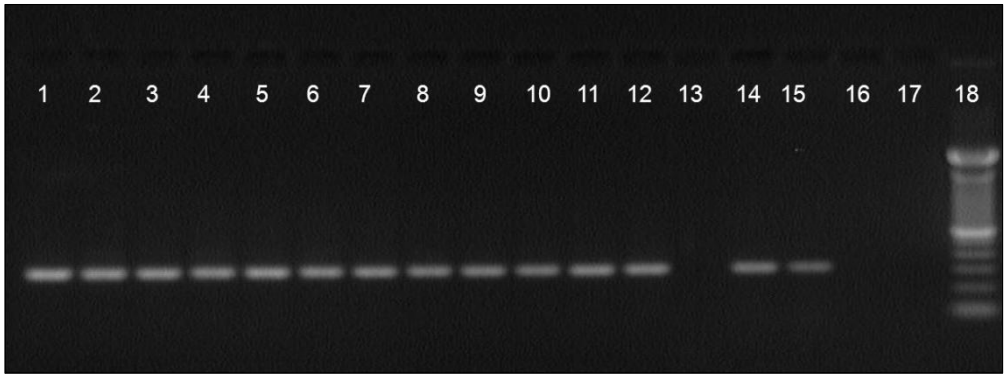

Figure 8. Amplicon of PBGD on agarose gel electrophoresis. All samples showed the expected size of the product (313bp). PCR products separated from untreated and treated prostate cancer cell lines DU-145 and LNCaP (from experiments 1 to 3, see chapter 2.2.2; lanes 1-12), no template control (NTC, lanes 13), controls from two prostate cancer tissue cDNAs (lanes 14-15), 16-17 empty lane, and 100bp DNA ladder (lane 18).

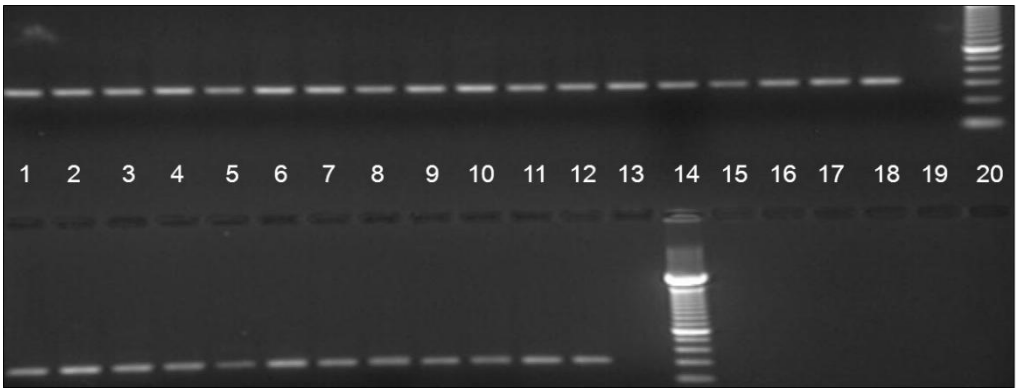

Figure 9. Amplicon of PBGD on agarose gel electrophoresis. All samples showed the expected size of the product (313bp). PCR products separated from the adjacent normal and tumor prostate tissue samples cDNA. Above: 1-9 paired samples (lanes 1-18), no template control (NTC, lane 19), and 100bp DNA ladder (lane 20). Below: separated PCR products from 44-50 paired PCa samples (lanes 1-12), no template control (NTC, lane 13) and 100bp DNA ladder (lane 14).

Table 3. Protocol of amplicon synthesis procedure

Components	Volume	Concentration
Template cDNA	1µL	10-50ng/20µL
Buffer (x10)	2µL	-
$MgCl_2$ (25mM)	1.6µL	2mM
dNTPs (2,5mM)	1.6µL	0.2mM
Upstream-Primer (10µM)	0.4µL	0.2µM
Downstream-Primer (10µM)	0.4µL	0.2µM
Enzyme	0.2µL	-
H_2O	12.8µL	-
Total volume	20µL	

Table 4. Cycling protocol of amplicon synthesis

Program	Conditions	
	Temperature	Time duration [min]
Pre-incubation	95°C	15:00
Amplification (35 cycles)	95°C	00:30
	60°C	00:30
	72°C	00:30
Extension time	72°C	07:00
Cooling	4°C	∞

Amplification primers for the various target genes were also provided by TIB MOLBIOL Berlin. Reaction components and cycling condition for both reactions are presented in tables 3 and 4.

2.2.9 Quantitative real-time PCR (RT-qPCR)

Real-time qPCR instruments were used to quantify the accumulation of newly synthesized cDNA strands at every PCR. A quantitative fluorescence signal was gathered either directly with intercalating dyes to the double stranded DNA, or indirectly with so-called hybridization or hydrolysis probes. These were dye-labeled oligonucleotides that specifically bind to one stand of the amplicon. UPL probes used in our protocols are short locked nucleic acids (LNAs) that behave like hydrolysis probes in PCR amplifications and are a trademark of Roche Diagnostics GmbH. One major advantage of using UPL technology is the application of one unique PCR protocol that allows many different targets to be amplified in one instrument run [68].

RT-qPCR was performed on the LightCycler 480 instrument with software version 1.5.0 in white 96-well PCR-plates. 1µL cDNA was amplified using the Probe Master kit, UPL probes from Roche Diagnostics GmbH (Mannheim, Germany) and primers from TIB MOLBIOL (table 7),with a total volume of 10µL (table 5). The cycling condition consisted of pre-incubation at 95°C for 10 minutes, followed by 45 amplification cycles at 95°C for 10 seconds, 59°C for 30 seconds, 72°C for 1 second and at the end 1 cooling cycle at 40°C for 30 seconds (table 6).

Table 5. Protocol of reaction mix using cDNAs and LightCycler480 Probes Master kit

Components	Volume	Concentration
H_20	3.4µL	
Upstream-Primer (10µM)	0.25µL	10µM
Downstream-Primer (10µM)	0.25µL	10µM
Probe (Universal Probe Library)	0.1µL	
Master Mix (2 x conc.)[1)]	5µL	1x
cDNA template	1µL	
Total volume	10µL	

[1)]2× conc., ready-to-use hot-start PCR mix, contains FastStart Taq DNA Polymerase, reaction buffer, dNTP mix (with dUTP instead of dTTP), and 6.4 mM $MgCl_2$.

Table 6. Cycling protocol for relative quantification on LC480

Program	Temperature	Hold
Pre-incubation (1 cycle)	95°C	10:00 min
Amplification (45 cycles)	95°C	00:10 sec
	59°C	00:20 sec
	72°C	00:01 sec
Cooling (1 cycle)	40°C	00:30 sec

For each cycle, Mono-color FAM fluorescence measurements with wave lengths of 483-533nm were used.

The analytical precision of the RT-qPCRs (i.e. the standard deviation of the Cq values) was tested by intra-run (n=10) measurements for the gene FABP6. Cq values ranged between 22.65 and 22.78 with median-22.67, SD±0.044, and SD% 0.19.

Primer and probe sets were designed at the Roche Applied Sciences Homepage (http://www.roche-applied-science.com/sis/rtpcr/upl/ezhome.html). For detection of reference gene PBGD, HPRT1 and TBP expression, commercially available mRNA-specific (Roche) reference genes ready to use assays were used.

Table 7. Primers and UPL probe for target gene

Gene name with accession number	Forward primers Sequence 5' → 3'	Reverse primers Sequence 5' → 3'	UPL probe	Amplicon (nt)
GADD45A NM_001924.3	TTTGCAATATGACTTTGGAGGA	CATCCCCCACCTTATCCAT	19	72
ASNS NM_183356.2	GATGAACTTACGCAGGGTTACA	CACTCTCCTCCTCGGCTTT	2	70
POTEF NM_001099771.2	CGGCCAGAGTGGTAGAAATG	GCGTACCACAGGTGATTCCT	19	106
SARS NM_006513.2	TGGGCAAACCAAGAAGATG	GCAGATGGTACGGGTAGTGG	39	85
ABLIM3 NM_014945.2	GGCTCCCAAGCACTTTCA	ACCATGCCGTTTGTAGATCG	33	76
IFI6 NM_022873.2	CTGTGCCCATCTATCAGCAG	GGGCTCCGTCACTAGACCTT	41	75
SPRY4 NM_030964.3	CCCCGGCTTCAGGATTTA	CTGCAAACCGCTCAATACAG	17	85
CTH NM_001902.5	CCGTTCTGGAAATCCCACTA	TGAAGCAAAGGCCAAACAG	59	85
GSTP1 NM_000852.3	TCTCCCTCATCTACACCAACTATG	AGGTCTTGCCTCCCTGGT	56	114

To reduce analytical variation in general and inter-assay variation in particular, normal and tumor samples were always analyzed on the same PCR plate. No-template controls (NTC), standard and calibrator interplate controls were included in each PCR run. All samples were measured as duplicates or triplicates.

2.2.10 Standard curve generation

For the generation of standard curves, PCR products and cDNAs from normal and tumor tissue samples were mixed in a 1:1 ratio. This mixture was serially diluted (1:10) five times. All samples were run in duplicates and triplicates. LC480 instrument's integrated software calculates the PCR efficiency (E). Ideally, a PCR runs on E=2.0 [68]. The efficiency of PCR runs for our candidate genes varied from 1.84 to 1.96 (92-98%) and for reference genes from 1.81 to 1.95 (90.5-97.5%). For Cq calculation we set up the instrument for the "second derivative maximum" method. All calculations with regard to the PCR quality (e.g. E, slopes, intercepts, errors of the regression lines of the calibration curves) were done by internal software (tables 8 and 9).

Table 8. PCR quality of candidate genes

	SARS	GSPT1	GADD45A	SPRY4	ASNS	POTEF	ABLIM3	CTH	IFI6
Efficiency	1.87	1.96	1.84	1.94	1.95	1.84	1.95	1.93	1.91
Slope	-3.66	-3.413	-3.773	-3.468	-3.427	-3.772	-3.435	-3.493	-3.54
Y-intercept	16.71	20.51	18.60	18.61	22.10	16.74	16.72	15.71	20.1
Error	0.006	0.1	0.02	0.0004	0.05	0.02	0.03	0.01	0.03

Table 9. PCR quality of reference genes

	HPRT1	PBGD	TBP
Efficiency	1.92	1.81	1.95
Slope	-3.531	-3.869	-3.436
Y-intercept	22.55	16.98	11.50
Error	0.01	0.01	0.01

2.2.11 Reference gene selection

The suitability of housekeeping genes was checked with the program qBase^{PLUS} (Biogazelle, Belgium). The purpose was to select the most stable gene or combination of stable genes for normalization.

2.2.12 Normalization of RT-qPCR data

The mRNA expression levels of genes measured with PCa cell line samples were normalized using the ΔΔCq method [69] with efficiency correction by Pfaffl [70]. Supportive excel spreadsheets were provided by the website www.gene-quantification.info.

The following formula was used for normalization:

$$Ratio = \left(E1_{target}\right)^{\Delta CT(control-treated)} \Big/ \left(E2_{reference}\right)^{\Delta Ct(control-treated)}$$

Specific mRNA expression of prostate tissues was normalized using GenEx software (www.multid.se). The so-called "$2^{-\Delta\Delta Cq}$ method" is implemented in this software and uses the following formula for calculations:

1) Interplate normalization:

$$Cp_{Interplatenorm} = Cp - \frac{1}{n}\sum_{i=1}^{n} Cp_{IC}$$

2) Efficiency correction:

$$Cp_{E=100\%} = Cp_{E}\frac{\log(1+E)}{\log 2}$$

3) Normalization of candidate genes (CG) to reference gene (RG):

$$Cp_{CG,norm} = Cp_{CG} - \frac{1}{n}\sum_{i=1}^{n} Cp_{RG}$$

4) Tumor to normal ratio:

$$Ratio^{T}/_{N} = 2^{-Cp(Tumor)+Cp(Normal)}$$

2.2.13 Computational analyses

At a certain point of the workflow, data provided by special websites, such as Serial Analysis of Gene Expression (SAGE) and CpG island detection, were included to rationalize future experimental work.

2.2.13.1 CpG island detection

The region of genes containing a high frequency of cytosine (C) and guanine (G) dinucleotides are called CpG islands (CpG) [56]. If this accumulation of methylated CpGs occurs in eukaryotic promoters, this phenomenon is called promoter hypermethylation [49]. Usually promoter hypermethylation goes along with a downregulation of that particular gene. Internet-based software EMBOSS CpGPlot provided by the European Bioinformatics Institute (EBI) (http://www.ebi.ac.uk/Tools/seqstats/emboss_cpgplot/) is one software tool that can be used to detect CpG islands of upregulated genes. We checked all our candidate genes for the presence of such CpG islands.

2.2.13.2 Serial Analysis of Gene Expression-(SAGE) Anatomic Viewer

Candidate genes expression status was checked online using Serial Analysis of Gene Expression-(SAGE) Anatomic Viewer software provided by the National Cancer Institute (NCI) website (http://cgap.nci.nih.gov/SAGE/). Color-coded scheme (figure 10) helps to discriminate expression level of the particular transcript in question between normal and tumor prostate tissues [71]. Suitable candidates should be elevated in normal tissue or at least display equal expression levels in normal and tumor tissues.

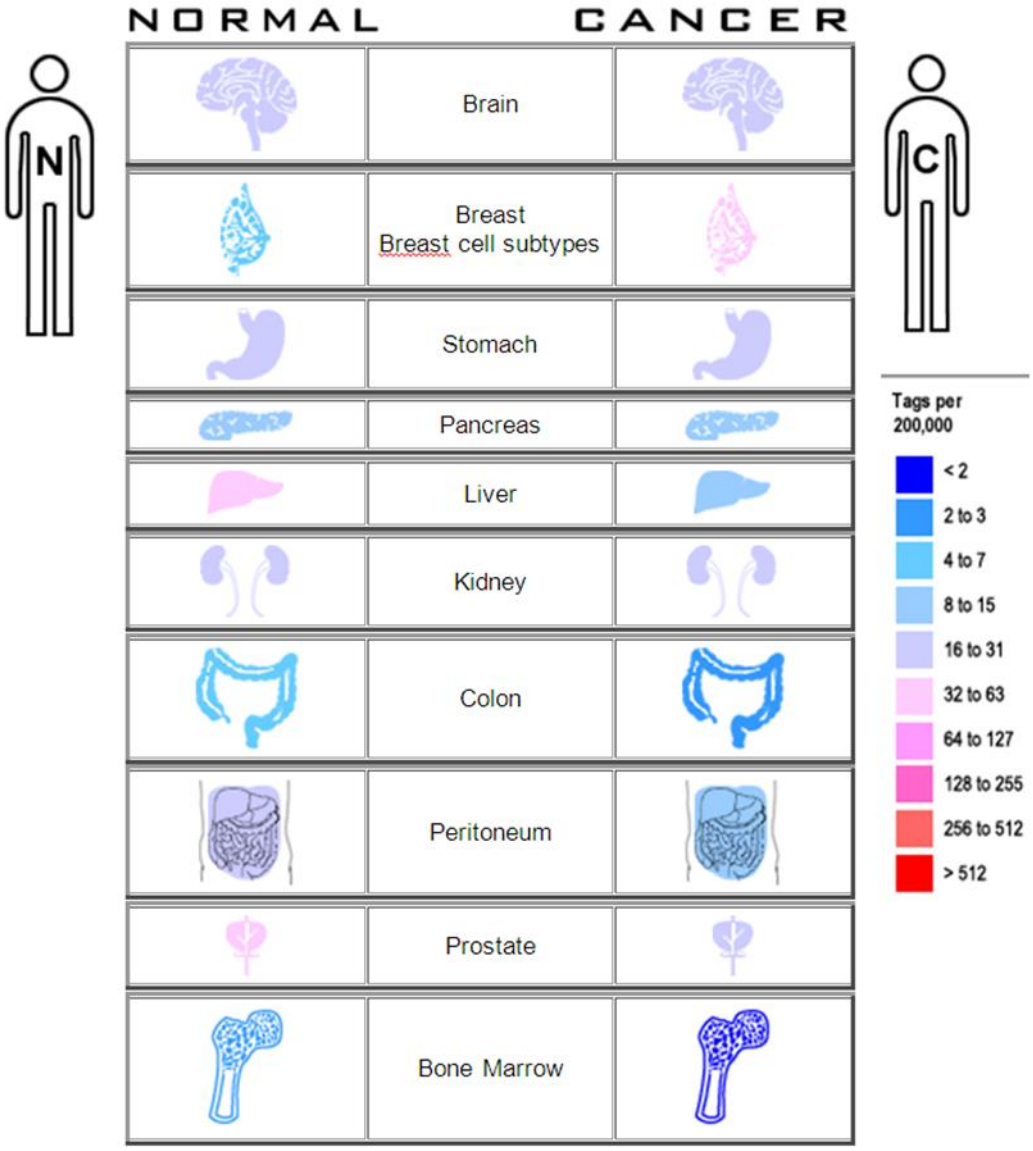

Figure 10. Expression profile for gene SARS as provided by SAGE anatomic viewer. According to the color scale, there is a clear upregulation in normal prostate tissue (32 to 63) over the cancer tissue (16 to 31).

2.2.14 Statistical evaluation

Statistical evaluation of RT-qPCR data was performed with the GraphPad Prism version 5.01 (GraphPad Software Inc., La Jolla, CA) software. The D'Agostino-Pearson omnibus normality test was used to identify the quantity of deviation from Gaussian distribution. Differences in gene expression between adjacent normal and tumor tissues were analyzed using the Wilcoxon test, Mann-Whitney *U* test, and Spearman rank correlation coefficients. All *p*-values <0.05 were considered statistically significant. To determine the discriminative potential of deregulated genes between normal and tumor

samples and the diagnostic accuracy, we used receiver operating curves (ROC) calculated by MedCalc software version 9 (MedCalc Software, Mariakerke, Belgium). The performance of the diagnostic variables was quantified by calculating the area under the ROC curve (AUC), P-value and confidence interval for AUC. The sample size (α error=5%, power=80%) for the comparison of the AUC of 0.8 (taking into account this value as appropriate discrimination power) with the null hypothesis value 0.5 was calculated to be 28 in each group. Ratio of expression and Youden's index were chosen as cut-off for dichotomize the ratio of adjacent normal and tumor sample expression. Overall survival and disease progression were calculated as a function of gene of interest (ASNS, GADD45A, SARS, SPRY4) using the Kaplan-Meier analyses with the log-rank test on SPSS version 19 (SPSS, Inc., an IBM Company, USA). Disease progression as primary clinical endpoint was defined as months elapsed between operation and biochemical relapse and overall survival time between operation and the last follow-up date. In total, our study comprised 50 patients, among them: 4 deceased patients. For 7 patients, no follow up data were available.

3 Results

3.1 Patient sampling and clinical characteristics

Samples of tumor tissue and adjacent normal tissue of 50 patients with a median age of 64 years and a median PSA level of 8.7ng/ml who underwent radical prostatectomy at the Charité - Universitätsmedizin Berlin were selected randomly for this study. Most of the patients had a staging of pT2b, pT2c, pT3a, or pT3b (92%) and Gleason scores varying from 5 to 7 (80%). None of patients had distant metastases, although 6 patients were defined pN1 (lymph node positive). The follow-up time ranged from from 1-131(median 104) months and follow-up was missing for 7 patients. Nine patients (18%) had biochemical recurrence. Clinical and histopathological data of all patients are given in table 10 below. Adjacent normal and tumor prostate tissue samples were exclusively used for total RNA extraction followed by additional biochemical analyses as described in the Materials and Methods section.

Table 10. Patients clinical characteristics

Characteristic	Parameters	Patients n=50 (100 %)
Age, years	Median	64
	Range	47- 74
Pre-operative PSA, ng/ml	Median	8.7
	Range	1.06- 78
pT stage	pT2a	1 (2)
	pT2b	15 (30)
	pT2c	12 (24)
	pT3a	6 (12)
	pT3b	13 (26)
	pT3x	1 (2)
	pT4	2 (4)
N stage	N0/Nx	44 (88)
	N1	6 (12)
M stage	M0	50 (100)
Gleason score	n/a	1 (2)
	3	1 (2)
	5	15 (30)
	6	12 (24)
	7	13 (26)
	8	4 (8)
	9	4 (8)
Follow-up, months		1-131
Follow up missing patients		7 (14)
Biochemical recurrence		9 (18)

All data obtained from patients' discharge papers available at \\Charite.de\Centren\C08\UR\#Public\Alte-Briefe for qualified personnel only.

3.2 Cell treatment

The PCa cell lines DU-145 and LNCaP were treated with zebularine at a concentration 100µM for 10 days. No obvious antiproliferative or cytotoxic effects, such as massive detachment and rounding the shape of cells, were detected during the entire zebularine exposure. The morphology of the cells was documented photographically (figure 11).

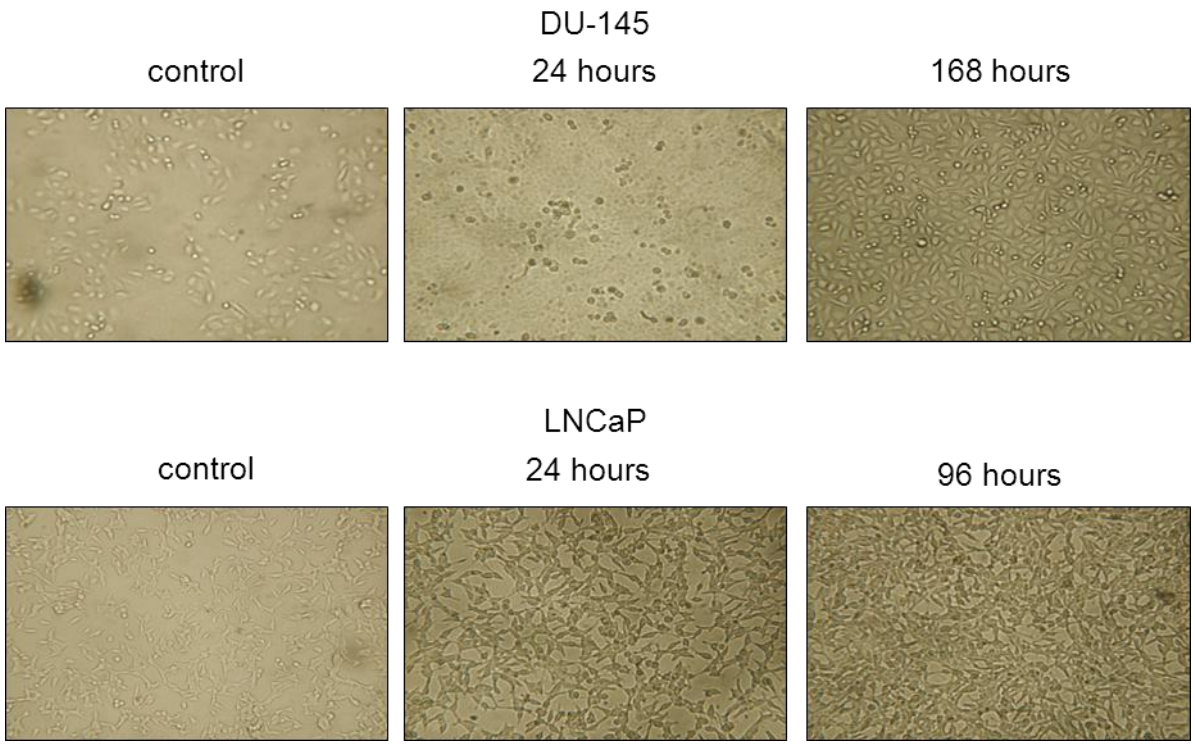

Figure 11. Microscopic observation (10x magnifications) of proliferation of prostate cancer cells DU-145 and LNCaP. Growth behavior after the treatment with 100µM of zebularine.

3.3 XTT cell proliferation assay

The XTT cell proliferation assay is a useful tool for the spectrophotometric quantification of cell proliferation and viability in response to zebularine. The experiments were carried out according to the manufacturer's instructions and were aimed to detect the effective concentration of zebularine with regard to its demethylating potential. The data are presented as percentage of inhibition of cell proliferation at different concentrations of zebularine (0–10–30–100–300–1000µM) after 48, 72 and 96 hours. We observed at all concentrations used that LNCaP cells were more sensitive to zebularine when compared to the DU-145 cell line. The proliferation of cells was decreased at higher concentrations of zebularine in both cell lines and varied depending on the exposure periods (48, 72, 96 hours) between 40-80% in LNCaP and 70-110% in DU-145. 100µM of zebularine was determined as the optimal concentration for the treatment of both cell lines. The proliferation of cells at this concentration was between 60-80% in LNCaP and 90-110% in DU-145 (figure 12).

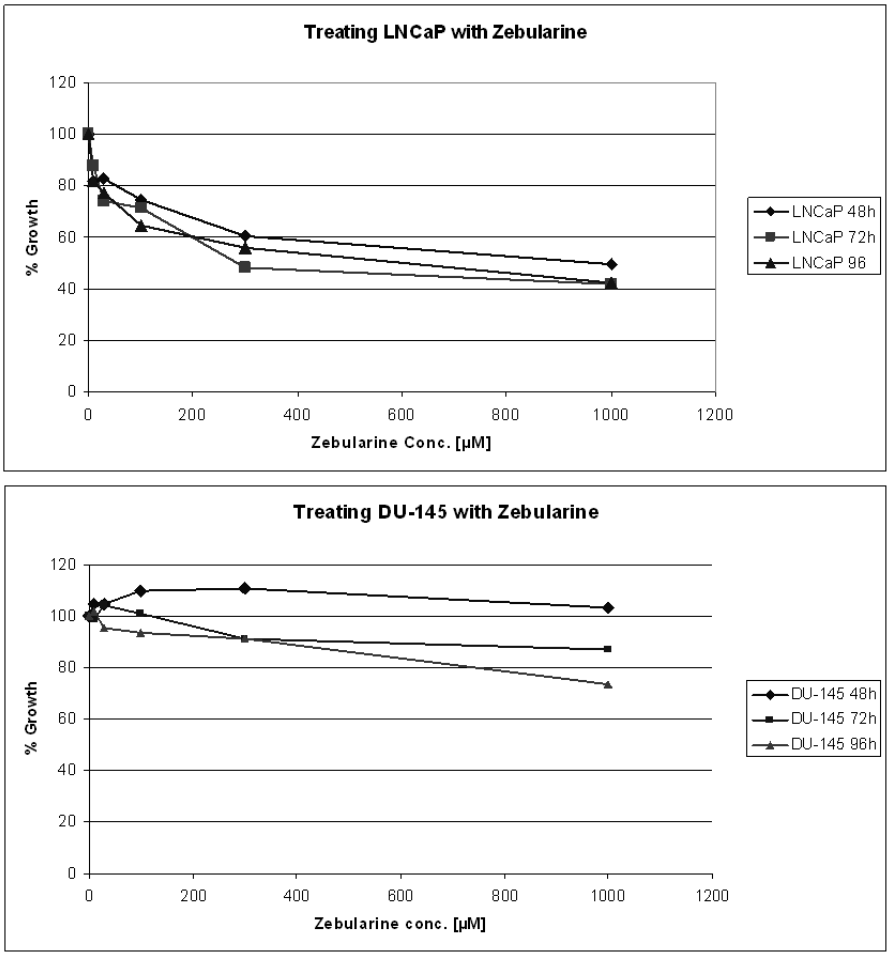

Figure 12. XTT test of LNCaP and DU-145 cells. Cells after 48, 72 and 96 hours of treatment with different concentrations of zebularine (0–10–30–100–300–1000µM).

3.4 Morphological assessment of apoptosis by fluorescent microscopy

The following experiments were aimed to differentiate between viable, apoptotic and necrotic cells. For this purpose we stained the cultures with an equal molar mixture of acridine orange/ethidium bromide after the cells had been treated for 48 to 96 hours with zebularine in concentrations of 0µM, 100µM, and 200µM. Photographic documentation was carried out at 10x and 20x magnification (figure 13). There were no differences between the cells treated with concentrations of 100 µM and 200 µM at exposure times from 48 to 96 hours.

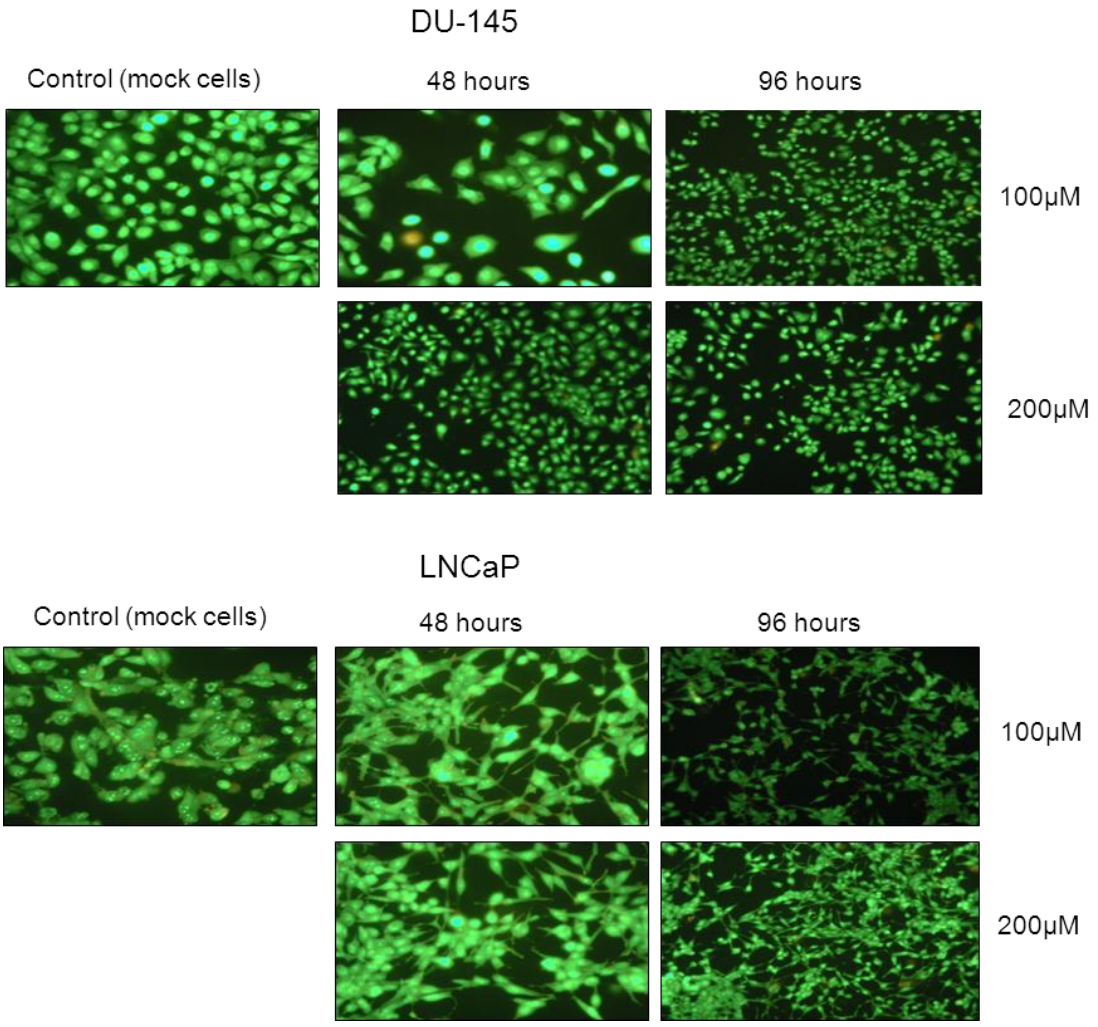

Figure 13. Fluorescence photography of prostate cancer cell lines DU-145 and LNCaP after staining with acridine orange/ethidium bromide.

3.5 RNA quantity and quality control

All tissue and cell culture RNA samples were examined for their concentration, purity and integrity. Treated and untreated DU-145 and LNCaP RNA samples (mean concentrations: 547.5ng/µL; 634.6ng/µL) with higher RIN values (9.8±0.1; 8.4±0.8) and absorbance ratios of 260/280nm (mean±SD: 2.0±0.008; 2.0±0.02), and 260/230nm (mean±SD: 2.2±0.1; 2.2±0.03) were selected for microarray analysis. The non-malignant and malignant RNA samples (mean concentration: 713.2ng/µL and 969.2ng/µL) based on the absorbance ratios of 260/280nm (mean±SD: non-malignant 2.0±0.03; malignant 2.0±0.02) and 260/230nm (mean±SD: non-malignant and malignant 2.1±0.1) were pure and protein-free. The RIN numbers (mean±SD) for non-malignant and malignant samples were 7.6±0.6 and 7.8±0.8, respectively.

3.6 Verification of treatment efficacy

In our experiments, we wanted to determine the efficacy of zebularine with regard to its demethylating potential. Instead of using e.g. direct bisulphite sequencing of genomic DNA (i.e. marking single mC conversions on the nucleotide level), we chose an indirect measurement, i.e. the zebularine-driven upregulation of transcripts known to harbor promoter CpG islands and to be regulated by promoter methylation. We chose the actin binding LIM protein family member 3 (ABLIM3) for the DU-145 model and interferon alpha-inducible protein 6 (IFI6) in the case of LNCaP cells (figure 14), respectively. This presumed upregulation after treatment with zebularine was measured on the RNA level with RT-qPCR.

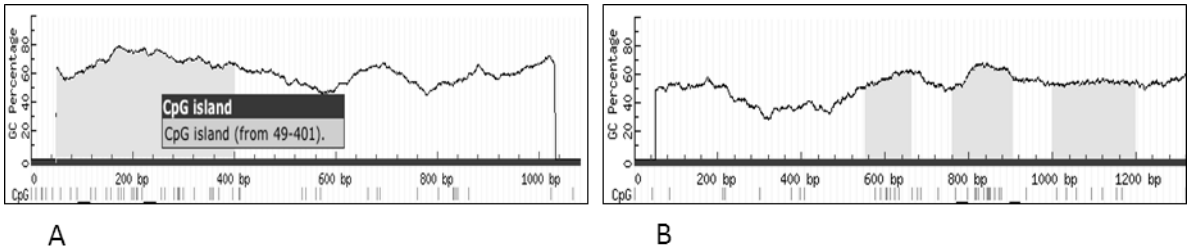

Figure 14. CpG island plots of ABLIM3 (A) and IFI6 (B). Predicted CpG islands are shown in grey boxes.

For relative quantification, 1µL cDNA was amplified; using the Probe Master kit and the UPL probe from Roche Diagnostics GmbH, the relative gene expression (RGE) was measured in triplicates. HPRT1 was used as reference gene to normalize gene expression. The target genes IFI6 and ABLIM3 from the treated cell's RNA showed a remarkable upregulation of three Cq values over the untreated cell's RNA from 27.58 to 23.92 and 32.22 to 28.00, respectively (figure 15, tables 11 and 12). As expected, the reference gene showed no difference in expression/regulation in either treated or untreated cells.

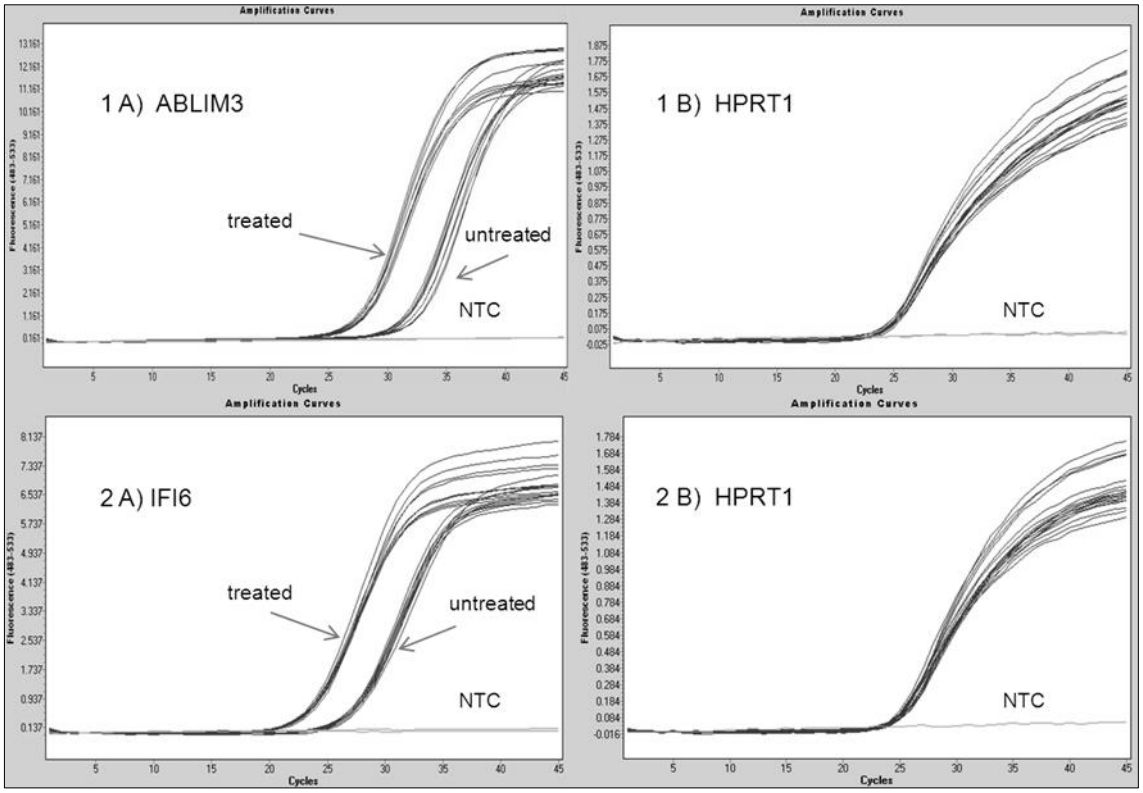

Figure 15. LightCycler480 RT-qPCR run for the ABLIM3 (1A) and IFI6 (2A) genes and the reference gene HPRT1. Visual differences are seen in both gene expressions by a shift from higher (mock) to lower Cq values after zebularine treatment (1A; 2A). Reference gene Cq values remain the same in both treated/untreated cells (1B; 2B).

The RGE expressed as a ratio based on the expression of target to reference gene between untreated and treated cancer cells was determined by using the ΔΔCq method [69], including efficiency correction by the Pfaffl et al. method [70] (tables11 and 12).

Table 11. RGE calculated according to the Pfaffl et al. method for the gene IFI6 with reference gene HPRT1 in three independent experiments

Gene IFI6	**Untreated**		**Treated**		**Target**	**Pfaffl top**	**Control (ref. gene)**	**Pfaffl bottom**	**RGE**
LNCaP	HPRT1	IFI6	HPRT1	IFI6	ΔCq	E1	ΔCq	E1	E1/E2
1 exp	24.65	27.45	25.12	23.88	3.57	11.88	-0.46	0.73	16.34
2 exp	24.55	27.45	24.93	24.09	3.36	10.27	-0.38	0.77	13.36
3 exp	24.35	27.84	25.12	23.77	4.07	16.80	-0.77	0.59	28.64
mean	24.52	27.58	25.06	23.92	3.67	12.73	-0.54	0.69	19.4

Table 12. RGE calculated according to the Pfaffl et al. method for the gene ABLIM3 with reference gene HPRT1 in three independent experiments

Gene ABLIM3	Untreated		Treated		Target	Pfaffl top	Control (ref.gene)	Pfaffl bottom	RGE
DU-145	HPRT1	ABLIM3	HPRT1	ABLIM3	ΔCq	E1	ΔCq	E1	E1/E2
1 exp	24.69	32.23	24.47	27.89	4.33	20.11	0.23	1.17	17.15
2 exp	24.32	32.57	24.40	27.90	4.67	25.46	-0.08	0.95	26.91
3 exp	24.35	31.86	24.53	28.22	3.64	12.47	-0.18	0.88	14.12
mean	24.45	32.22	24.46	28.00	4.22	18.64	-0.01	0.99	19.3

The calculated mean of upregulation for the gene ABLIM3 was 19.3-fold (SD±3.8), whereas the mean average for upregulation of the gene IFI6 was 19.4-fold (SD±4.6).

3.7 RNA microarray expression data

Principal component analysis (PCA) and hierarchical clustering of microarray data revealed that the treated and untreated samples clustered according to their division and groups and that we could clearly separate them from each other (figure 16).

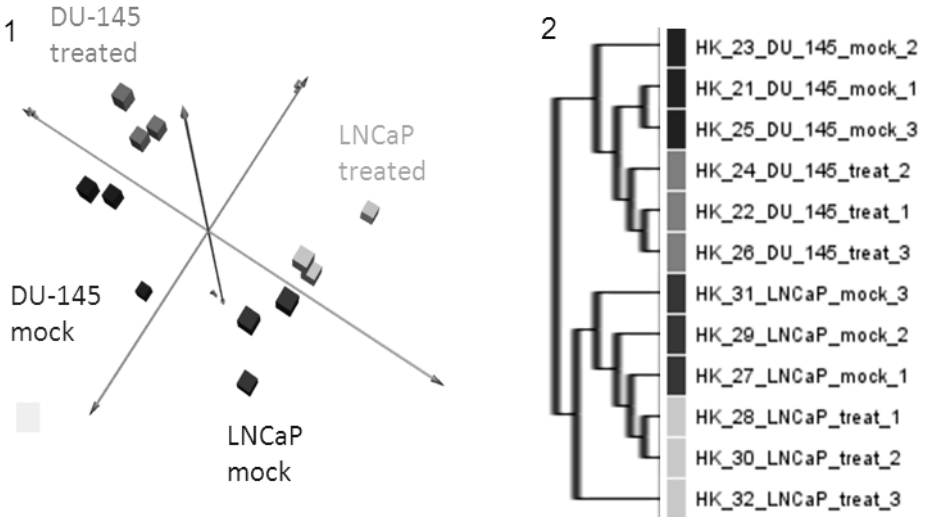

Figure 16. 1) Principal component analysis (PCA) 2) Hierarchical clustering (average linkage clustering). Clustering of prostate cancer cell lines DU-145 and LNCaP after the treatment with the DNMT inhibitor zebularine.

In the next step of RNA microarray data analysis, the differential expression on 21014 human genes between untreated and treated cells revealed in total 3447 genes expressing at least ≥1.5-fold in 3 experiments in both cell lines. The number of probe sets that shared ≥1.5-fold change of upregulation was analyzed by using Venn diagrams. The numbers of ≥1.5-fold change upregulated genes were 85 and 31 in DU-145 and LNCaP, respectively (figure 17).

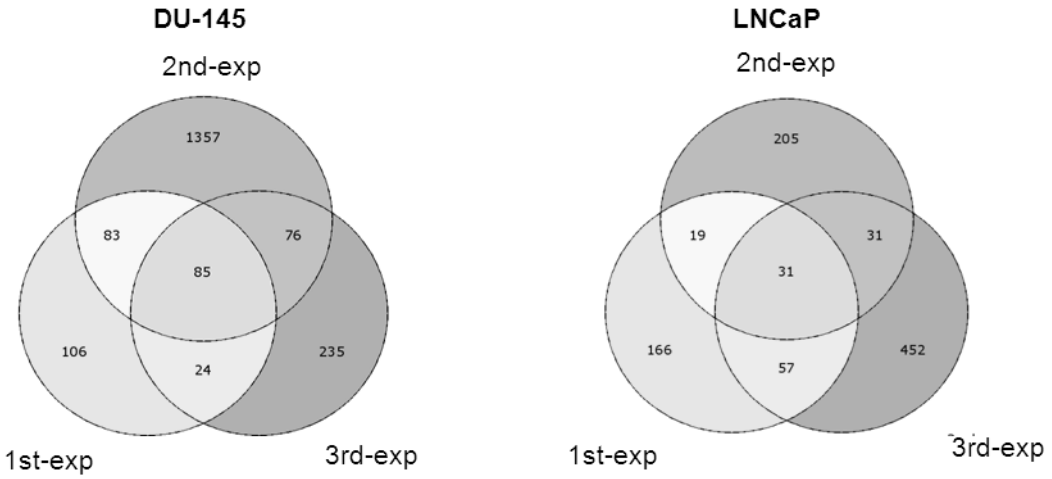

Figure 17. Number of shared ≥1.5 fold upregulated genes in Venn diagrams in the three independent biological experiments in PCa cell lines DU-145 and LNCaP after treatment with the demethylating (DNMT) agent zebularine.

The number of genes was decreased by removing duplicate values and by choosing the genes that were upregulated ≥2 fold. A total 91 genes were at least 2-fold upregulated in the two PCa cell lines.

3.8 Candidate selection

To narrow the list of suitable candidates, we applied several selection criteria that suitable candidates should fulfill. As a first criterion the presence/absence of CpG islands in the promoters of the respective genes was analyzed *"in silico"*. For this purpose genomic sequences of 5000nt upstream of the transcriptional start site (TSS) were downloaded from the NCBI database and analyzed with the CpG island prediction program "Emboss" provided by the EBI-EMBL Tools website. 63/91 (69.2%) of the genes, that is more than the two thirds of upregulated genes, harbor CpG island(s).

As a second criterion we analyzed the expression of our candidate genes online with the SAGE Analysis Viewer tool (see also chapter 2.2.14). Genes that had higher or equal expression in normal prostate tissue compared with PCa tissue were determined as the most preferred candidates for further analysis in patient samples. In 55/91 (60.4%) genes were equally regulated and in 19/91 (21%) genes were downregulated in tumor tissue. We focused on genes that displayed a higher expression in normal than in malignant tissue. By applying the two selection criteria we were chose these genes as candidates for methylation-dependent gene regulation. Accordingly, excluding genes without CpG islands and genes expressed preferentially in tumor tissue, we ended up with 51 genes that are listed in table 13. Their post-treatment expression increase (= fold-change) varied 2.01 to 4.86 with a median of 2.52.

Table 13. List of upregulated genes after bioinformatics analyses[1)]

Gene symbol[2)]	Gene name	Location	Fold change	CpG island[3)]	Digital Northern[4)]
ADRA2A	adrenergic, alpha-2A-, receptor	10q25.2	2.31	YES	D
DDX60	DEAD (Asp-Glu-Ala-Asp) box polypeptide 60	4q32.3	2.97	yes	S
POTEF	POTE ankyrin domain family, member F	2q21.1	2.15	yes	D
DDX58	DEAD (Asp-Glu-Ala-Asp) box polypeptide 58	9p12	3.75	yes	S
IGF1R	insulin-like growth factor 1 receptor	15q26.3	2.72	yes	S
INPP4B	inositol polyphosphate-4-phosphatase, type II	4q31.21	2.63	yes	D
IFI6	interferon, alpha-inducible protein 6	1p35	4.86	yes	D
TXNIP	thioredoxin interacting protein	1q21.1	4.65	YES	D
ADAM32	ADAM metallopeptidase domain 32	8p11.22	3.73	yes	S
STC2	stanniocalcin 2	5q35.1	3.68	yes	S
BEST1	bestrophin 1	11q13	3.63	YES	S
ASNS	asparagine synthetase (glutamine-hydrolyzing)	7q21.3	3.39	YES	D
CTH	cystathionase (cystathionine gamma-lyase)	1p31.1	3.36	yes	S
C12orf39	chromosome 12 open reading frame 39	12p12.1	3.19	YES	S
JHDM1D	jumonji C domain containing histone demethylase 1 homolog D (S. cerevisiae)	7q34	3.08	yes	S
PPP1R15A	protein phosphatase 1, regulatory	19q13.2	2.99	YES	S

	subunit 15A				
SPRY4	sprouty homolog 4 (Drosophila)	5q31.3	2.96	yes	S
ZC3H6	zinc finger CCCH-type containing 6	2q13	2.87	yes	S
TMEM156	transmembrane protein 156	4p14	2.87	yes	S
FAM129A	family with sequence similarity 129, member A	1q25	2.80	yes	S
CDRT1	CMT1A duplicated region transcript 1	17p12	2.74	yes	S
UPP1	uridine phosphorylase 1	7p12.3	2.71	yes	D
MAP2	microtubule-associated protein 2	2q34-q35	2.65	yes	S
MOCOS	molybdenum cofactor sulfurase	18q12	2.59	yes	S
C6orf48	chromosome 6 open reading frame 48	6p21.3	2.58	YES	S
PYROXD1	pyridine nucleotide-disulphide oxidoreductase domain 1	12p12.1	2.54	yes	S
ZNF814	zinc finger protein 814	19q13.43	2.52	yes	S
CLDN1	claudine 1	3q28-q29	2.52	yes	S
ABLIM3	actin binding LIM protein family, member 3	5q32	2.52	yes	D
DDIT4	DNA-damage-inducible transcript 4	10q22.1	2.51	YES	S
TFPI2	tissue factor pathway inhibitor 2	7q22	2.51	YES	S
TUBE1	tubulin, epsilon 1	6q21	2.45	yes	D
GADD45A	growth arrest and DNA-damage-inducible, alpha	1p31.2	2.36	YES	S
FRZB	frizzled-related protein	2qter	2.34	yes	S
C5orf28	chromosome 5 open reading frame 28	5p12	2.33	yes	D
SERPINB8	serpin peptidase inhibitor, clade B (ovalbumin), member 8	18q22.1	2.33	yes	S
ZNF300	zinc finger protein 300	5q33.1	2.32	yes	S
ZDHHC11	zinc finger, DHHC-type containing 11	5p15.33	2.29	yes	S
GTPBP2	GTP binding protein 2	6p21	2.27	yes	D
MKX	mohawk homeobox	10p12.1	2.24	yes	S
CD274	CD274 molecule	9p24	2.22	yes	S
ZNF643	zinc finger protein 643	1p34.2	2.19	yes	S
C9orf150	leucine rich adaptor protein 1-like	9p23	2.19	yes	S
TES	testis derived transcript (3 LIM domains)	7q31.2	2.17	yes	S
PSAT1	phosphoserine aminotransferase 1	9q21.2	2.16	yes	S
PAX6	paired box 6	11p13	2.15	yes	S
ETV5	ets variant 5	3q28	2.11	yes	S
SARS	seryl-tRNA synthetase	1p13.3	2.10	yes	D

CD226	CD226 molecule	18q22.3	2.04	yes	S
GDPD1	glycerophosphodiester phosphodiesterase domain containing 1	17q22	2.01	yes	S
LETM2	leucine zipper-EF-hand containing transmembrane protein 2	8p11.23	2.01	yes	S

[1)] Selected 51 genes that showed at least ≥2 fold upregulation in two prostate cancer cell lines.

[2)] Gene names **bold** were analyzed by RT-qPCR. Gene name *italic underlined* indicates gene previously identified as being hypermethylated in PCa but not analyzed by us. Gene names ***bold italic underlined*** indicate genes previously identified as being hypermethylated in PCa and analyzed in this project.

[3)] Upper and lower case letter indicate the size of CpG island(s): 'YES'=largest size and 'yes'=smallest size.

[4)] S-equally expressed in normal and malignant tissue, D-increased expression in normal prostate tissue.

3.9 Identification of suitable reference genes

Suitable reference genes should exhibit constitutive, nonregulated, stable expression in the investigated samples [72]. We used commercially available reference gene assays to detect the expression of the reference genes PBGD, HPRT1 and TBP. RT-qPCR was performed from 50 matched prostate adjacent normal and tumor tissue samples. The Cq values in HPRT1 ranged from 26.62 to 31.89 (mean: normal sample 28.88, SD±1.13; tumor sample 28.37, SD±1.02) and in TBP from 26.88 to31.93 (mean: normal sample 28.74, SD±1.14; tumor sample 28.29, SD±0.87). The Cq values in PBGD ranged from 27 to 34 (mean: normal sample 30.39, SD±1.3; tumor sample 29.39, SD±1.14).

The expression levels between nonmalignant and malignant samples were significantly different in all 3 reference genes (PBGD, $P<0.0001$; HPRT1, $P=0.002$; TBP, $P=0.0049$) (figure 18). Although, these genes were regulated, using geNorm^{PLUS} software we further analyzed them for reassessing their contribution as normalizer.

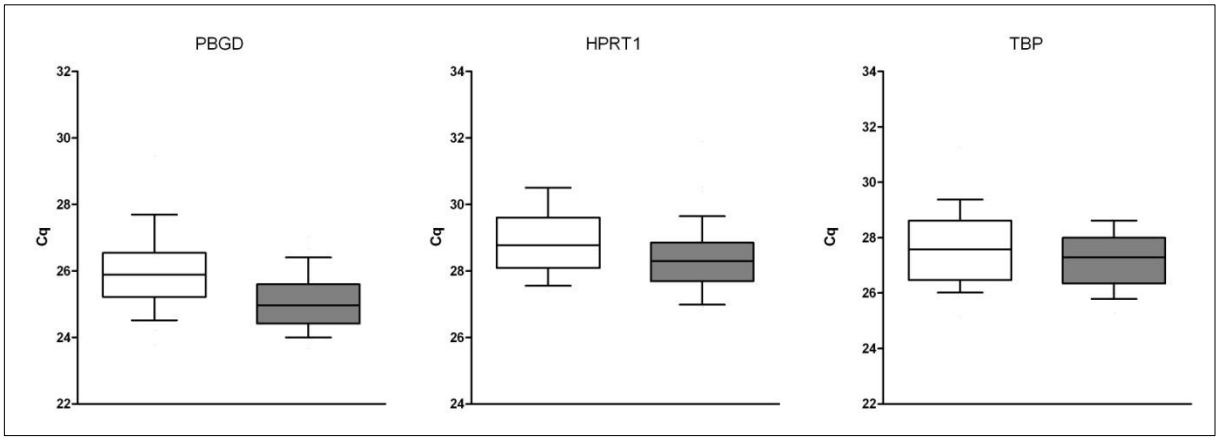

Figure 18. Expression of reference genes in prostate non-malignant and malignant tissue samples (white- nonmalignant; black-malignant). Whiskers show the 10-90 percentiles. Significance ($P<0.05$) was calculated using Wilcoxon signed rank test for PBGD, HPRT1 and TBP.

3.10 Evaluation of reference genes using geNorm^{PLUS}

To identify the most stable reference genes or combinations of them for the normalization, we applied the new computer program geNorm^{PLUS} an implementation of qBase^{PLUS}. GeNorm^{PLUS} allows candidate reference genes to be ranked up to the single most stable gene according to their M value, the gene with the highest M value being the least stable and the gene with the lowest M value being the most stable [73]. The gene with the most unstable expression level was TBP (M=0.810) and the most stable one was PBGD (M=0.5950). The average stability expression level showed HPRT1 (M=0.650) (figure 19).

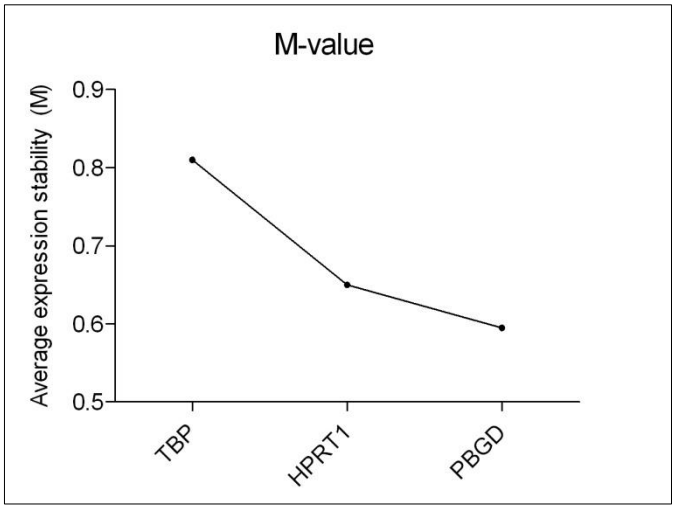

Figure 19. GeNorm^{PLUS} analysis of RT-qPCR data of candidate reference genes: Average expression stability (M). The gene with the highest M value on the left has the least stable expression (TBP) (M=0.810), while the gene with the lowest M value on the right (PBGD) (M=0.595) has the most stable gene. HPRT1 was in between and showed M=0.650.

The normalization factor (V_{NF} value) is the pairwise variation criterion for optimum number of reference genes for normalization with a cut off value of less than 0.15 [73, 74]. GeNorm^{PLUS} did not suggest any combination of genes and the most suitable reference genes combination V2/3 showed V_{NF}=0.26.

Ultimately, PBGD was selected for further normalization process of candidate genes expression.

3.11 Validation of differentially expressed target genes using RT-qPCR

After carrying out calculations and selecting reference genes, selected candidate genes were verified for downregulation/inactivation in tumorous tissues of human PCa. The expressions of a total of 9 genes including GSTP1 were detected by RT-qPCR from 50 matched prostate adjacent normal and tumor tissue samples on LightCycler480. The gene POTEF (P<0.0001) was significantly upregulated in tumor samples compared with adjacent normal ones. The Cq values in POTEF ranged from 27.24 to 39.60 (mean: normal sample 34.08, SD±2.26; tumor sample 31.71, SD±1.65).

The Cq values in CTH ranged from 24.02 to 31.66 (mean: normal sample 27.31, SD±1.55; tumor sample 26.49, SD±1.17), in IFI6 from 23.90 to 31.61 (mean: normal sample 27.65, SD±1.65; tumor sample 27.04, SD±1.52), in ABLIM3 from 29.15 to 37.97 (mean: normal sample 34.54, SD±1.75; tumor sample 34.12, SD±1.51). The gene expressions of CTH (P=0.48), IFI6 (P=0.28) and ABLIM3 (P=0.063) showed no

significant difference between adjacent normal and tumor samples (figure 20). Consequently, a further evaluation of the genes POTEF, ABLIM3, CTH and IFI6 was not conducted.

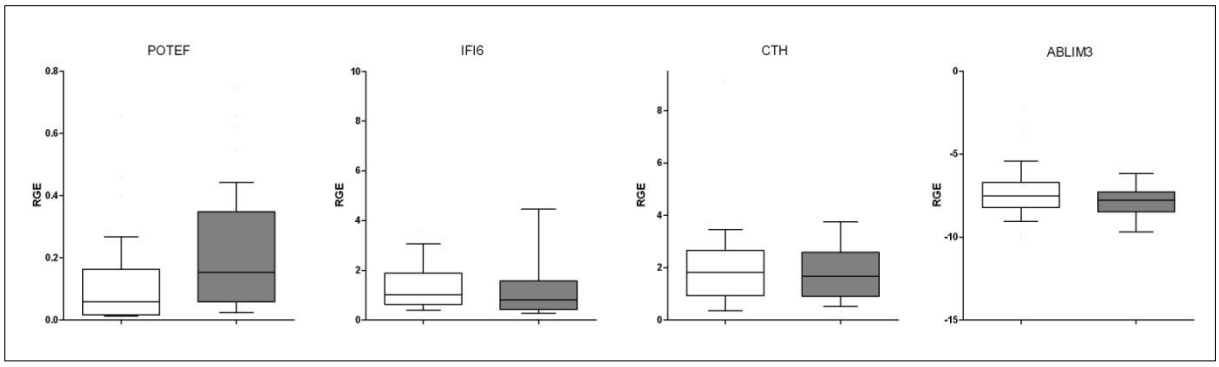

Figure 20. Expression of the candidate genes POTEF, IFI6, CTH, and ABLIM3 (expression $\log_2$ transformed) in prostate non-malignant and malignant tissue samples (white- nonmalignant; black-malignant). Whiskers represent the 10-90 percentiles. Significance (P<0.05) was calculated using the Wilcoxon signed rank test.

We were interested mainly in genes that were downregulated in tumor samples. The expression of genes GADD45A (P<0.0001), SARS (P<0.0001), SPRY4 (P=0.0007) and ASNS (P=0.0007) showed significant downregulation in tumor samples (figure 21). The Cq values in GADD45A ranged from 21.18 to 28.72 (mean: normal sample 25.61, SD±1.41; tumor sample 26.01, SD±1.17) and in SARS from 23.07 to 27.80 (mean: normal sample 24.92, SD±1.05; tumor sample 24.56, SD±0.90). The Cq values in SPRY4 ranged from 27.78 to 37.85 (mean: normal sample 31.85, SD±1.95; tumor sample 31.66, SD±1.81) and in ASNS from 24.84 to 28.84 (mean: normal sample 27.03, SD±0.78; tumor sample 26.53, SD±0.81). Tumor samples downregulation prevalence was 72% (36/50) for ASNS, 74% (37/50) for SPRY4, 88% (44/50) for GADD45A, and 84% (42/50) for SARS (table 14).

The gene glutathione S-transferase pi 1 (GSTP1) was included in the RT-qPCR analysis as hypermethylated and mainly suppressed in PCa [49]. The Cq values ranged from 19.74 to 25.11 (mean: normal sample 22.11, SD±1.07; tumor sample 22.67, SD±1.09). GSTP1 (P<0.0001) expression was also found to be significantly downregulated (90%; 45/50) in prostate tumor tissue samples.

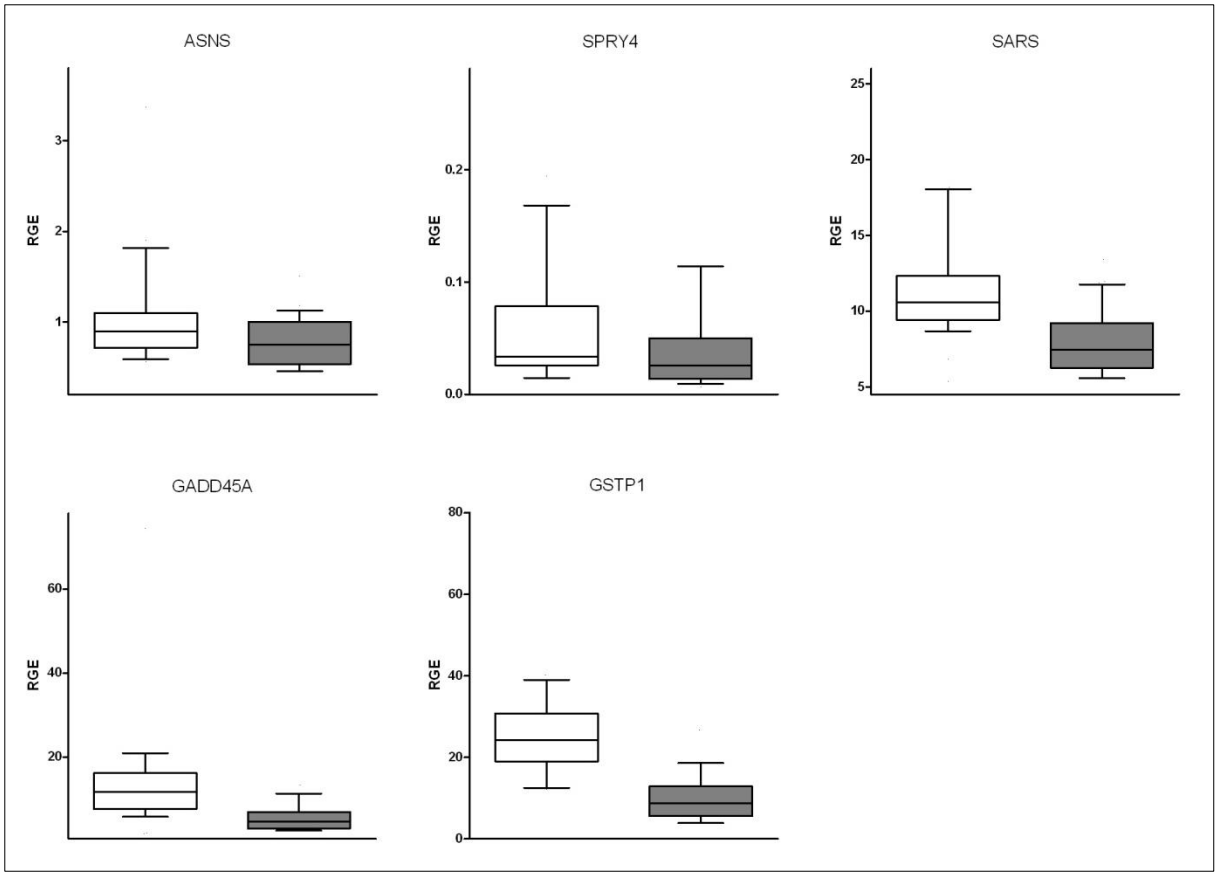

Figure 21. Expression of downregulated candidate genes ASNS, SPRY4, SARS, GADD45A and GSTP1 in prostate non-malignant and malignant tissue samples (white- non-malignant; black- malignant). Whiskers represent the 10-90 percentiles. Significance (P<0.05) calculated with Wilcoxon signed rank test for all genes. Data are given in table 14.

We calculated the fold changes representing expression differences for each candidate gene, in adjacent normal and tumor tissues. In the present work we used cut off ≥-1.5-fold changes that is relevant according to the study by Chen et al [75]. Among the downregulated samples, in the genes SPRY4 (median-1.64; 31/37), GADD45A (median -2.32; 37/44) and GSTP1 (median-2.54; 42/45) we detected ≥-1.5-fold changes in 84%, whereas in genes ASNS and SARS in 44% (median-1.28; 16/36) and 55% (median-1.44; 23/42), respectively (table 14).

Table 14. mRNA expression changes of candidate genes*)

Genes	P-value	Downregulation (normal vs. tumor)	Fold changes (normal vs. tumor)	≥-1.5 fold changes (normal vs. tumor)
ASNS	0.0007	72% (36/50)	-1.28	44% (16/36)
SPRY4	0.0007	74% (37/50)	-1.64	84% (31/37)
SARS	<0.0001	84% (42/50)	-1.44	55% (23/42)
GADD45A	<0.0001	88% (44/50)	-2.32	84% (37/44)
GSTP1	<0.0001	90% (45/50)	-2.54	84% (42/45)

*) Significance (P<0.05) calculated with Wilcoxon signed rank test for all genes.

3.12 Eligibility of expression data as putative diagnostic markers for prostate cancer detection

To estimate the diagnostic properties of selected candidates, receiver operating characteristic (ROC) curves were calculated for each downregulated gene. The higher the area under the curve (AUC value), the higher is the predictive discriminatory effect between tumor and adjacent normal samples.

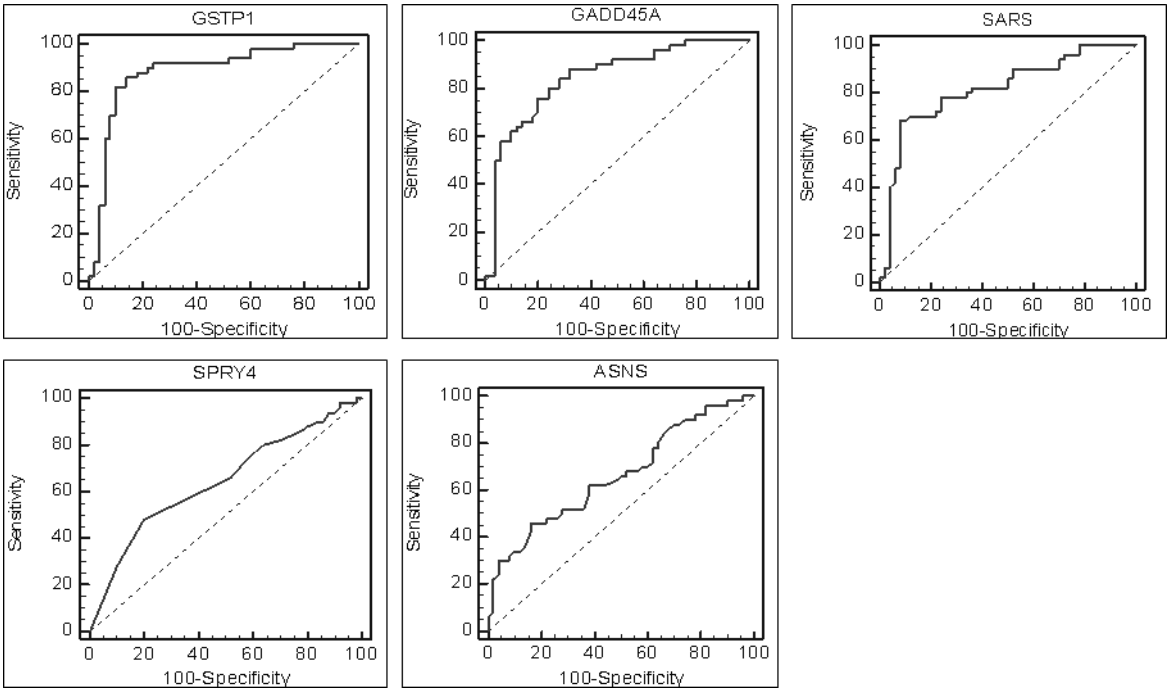

Figure 22. Receiver operating characteristic curve (ROC) for the significantly downregulated candidate genes GADD45A, SARS, SPRY4, ASNS and GSTP1 to discriminate between tumor and adjacent normal samples. Data are given in table 15.

ROC curves and calculated areas under the ROC curves (AUC) were comparable in shape and large in SARS (AUC=0.816), GADD45A (AUC=0.841), and GSTP1 (AUC=0.884) (figure 22, table 15). These genes showed a much better discrimination in comparison to ASNS (AUC=0.663; P=0.0026) and SPRY4 (AUC=0.644; P=0.0085) (figure 22, table 15). The specificity at a given 90% sensitivity reached a level of 78% for GSTP1, 58% for GADD45A, 48% SARS, 26% ASNS and 16% for SPRY4 (table 15). Additionally, we performed correlation analyses of expression data and clinical data.

Table 15. Receiver operating characteristic curve (ROC) for candidate genes*)

Gene	Sensitivity (95%CI)	Specificity (95% CI)	AUC	P-value	Standard error	Younden index
GSTP1	90% (78.2-96.7)	78% (64.0-88.5)	0.884	<0.0001	0.0369	14.98
GADD45A	90% (78.2-96.7)	58% (43.2-71.8)	0.841	<0.0001	0.0407	6.74
SARS	90% (78.2-96.7)	48% (33.7-62.6)	0.816	<0.0001	0.044	8.35
SPRY4	90% (78.2-96.7)	16% (7.2-29.1)	0.644	0.0085	0.0549	0.02
ASNS	90% (78.2-96.7)	26% (14.6-40.3)	0.663	0.0026	0.0543	0.64

*)Significance (P-value) and standard error of ROC analysis. Considered significances P<0.05. Youden index used as cut-off value to dichotomize expression ratios for further log-rank analysis.

3.13 Correlation of expression between candidate genes

We identified a strong positive correlation, with the regards to the ratio of mRNA expression, between GADD45A, GSTP1 and all other downregulated candidate genes (table 16). SARS also strongly correlated with all other genes, except SPRY4 (r_S=0.236, P=0.09) (table 16).

Table 16. Spearman rank correlation coefficients between downregulated candidate genes

Factor*)	SPRY4	ASNS	SARS	GADD45A	GSTP1
SPRY4	-	-0.101	0.236	0.428[b]	0.347[a]
ASNS	-0.101	-	0.642[c]	0.422[b]	0.387[b]
SARS	0.236	0.642[c]	-	0.591[c]	0.685[c]
GADD45A	0.428[b]	0.442[b]	0.591[c]	-	0.644[c]
GSTP1	0.347[a]	0.387[b]	0.685[c]	0.644[c]	-

*) Significantly downregulated candidate genes. Correlation coefficient (r_s) values and P-values are shown: [a]P<0.05; [b]P<0.01; [c]P<0.001.

GSTP1, GADD45A and SPRY4 play a key role in cancer prevention (table 17), since their functions comprise detoxification, apoptosis, DNA repair and cell cycle regulation, and all are downregulated by hypermethylation in PCa [49, 76, 77]. Besides the genes GADD45A and SARS are both located on the same chromosome (table 17). So far, there are no reports of SARS involvement in PCa or cancer in general.

Table 17. Characteristics of major candidate genes

Gene	Gene name	Gene function	Gene location
SPRY4	Sprouty homolog 4 (Drosophila)	Inhibition of the growth factor-induced cell responses by inhibiting the RTK-dependent Ras/MAP (mitogen-activated protein) kinase signaling pathway	5q31.3
ASNS	Asparagine synthetase (glutamine-hydrolyzing)	Aspartate and asparagine activity	7q21.3
SARS	Seryl-tRNA synthetase	Catalysis of the ligation of serine to tRNA	1p13.3
GADD45A	Growth arrest and DNA-damage-inducible, alpha	Regulation of cell cycle, DNA repair, apoptosis and inhibition of cell growth	1p31.2
GSTP1	Glutathione S-transferase pi 1	Cellular detoxification of xenobiotics and carcinogens	11q13

Gene name is the full gene name. Gene function and location were obtained from the GeneCard and PubMed database.

None of the expression data of our candidate genes showed a significant correlation with pathological parameters (TNM stage and Gleason score).

3.14 Stratification of expression ratios of candidate genes with pathological parameters

Accuracy in early diagnosis of PCa and its prognosis after radical prostatectomy is still a major challenge in clinical decision making. Clinical and pathological parameters such as the TNM stage, Gleason score, pre- and post-operative PSA value are used to categorize certain risk level groups (low, intermediate, and high) of PCa patients.

Performance of mRNAs expression as prognostic markers with dichotomized variables and pathological parameters (TNM stage and Gleason score) were analyzed by univariate Kaplan-Meier analysis. Initially, dichotomization was done according to median of ratio of expression. On the second effort, each gene ratio of tumor vs. normal expression was dichotomized according to their Youden index of ROC analysis (table 15).

4 Discussion

This thesis describes an experimental approach that exploits the ability of demethylating agents to reactivate transcriptionally silenced genes as a tool for the discovery of new biomarkers and putative therapeutic targets in prostate cancer [49]. The basic concept is built on the assumption that tumor suppressor genes are rendered inactive not only by genetic but also by epigenetic processes like promoter hypermethylation [27]. Any kind of treatment that converts the methylated status back to an (normal, i.e. non-tumorigenic) unmethylated one would therefore "unmask" silenced genes that may have contributed to respective tumorigenic events. Ideally, this demethylating treatment should be done in the tumor tissue under scrutiny. However, the majority of demethylating agents are inhibitors of DNA methyltransferases (DNMTs) that need active proliferation (several cell divisions) of the corresponding cells [78]. For this reason we chose two well-known PCa cell lines that differ in many aspects in their geno- and phenotype, especially in their status of the androgen receptor that is active in LNCaP and inactive in DU-145 cells. It should be noted that both cell lines were originally derived from metastases.

The experimental approach included:

- treatment of the respective cell lines with the demethylating agent zebularine including attempts to optimize efficacy (concentration, treatment time, proliferation status)
- a so-called "epigenetic screen" performed on total RNA extracts derived from treated and untreated cells. For this fundamental step in our approach, the three independent treatment experiments were conducted. The upregulated transcripts were initially identified by RNA chip technology.
- candidates for further investigation were selected by applying bioinformatics tools specifically aimed to handle methylation-related events
- selected candidate transcripts were eventually verified for their expression status in PCa patient tissue

The results obtained during these steps are discussed in the following chapters.

4.1 Epigenetic treatment and efficacy

By virtue of its chemical structure, zebularine belongs to the same group of pyrimidine analogs as its more frequently used relatives 5-Aza-CR and 5-Aza-CdR. Zebularine is known as a less toxic agent and has a more stable half-life in neutral solution when compared to other DNMT inhibitors [56, 60]. Several authors report that 5-Aza-CdR reduces cell proliferation and displays a non-negligible cytotoxicity at effective concentrations of 5-10µM [56, 79-81]. For example, Pulukuri et al. [79] reported a 70% inhibition of cell proliferation at a concentration of 10µM of 5-Aza-CdR [79], whereas Walton et al. [80] reported an inhibition of approximately 30% at concentration 8.8µM of 5-Aza-CdR. Chiam at al. [60] observed a significant reduction of the number of viable cells at zebularine concentrations of 100µM and 200µM. However, our experimental work did not show remarkable differences between control cells and cells treated at the same concentrations and exposure times (figure 11 and 13).

We placed particular emphasis on the efficacy of zebularine action, since this drug is known to be less active when compared to other demethylating agents. In addition, in clinical studies zebularine was found to be not as effective as 5-azacytidine [57, 58]. Other studies underline its suitability as a therapeutic agent [56, 59]. In experimental settings involving demethylation of the glutathione S-transferase π1 (GSPT1) promoter region, zebularine was found to be a weaker demethylating agent when compared to 5-Aza-CdR [60]. Generally, post-treatment GSTP1 activation is therefore considered as a good indicator to assess the effect of DNMT inhibitors in PCa [60]. In our experiments there was no difference in GSTP1 RNA expression between treated and untreated cells (data not shown). However, genes like GADD45, SPRY4, and TXNIP also known to be regulated by promoter hypermethylation, were clearly upregulated in our RNA microarray analyses (table 13) [76, 77, 82, 83].

Besides, principal component analysis (PCA) and hierarchical clustering of our microarray data analyses showed that the treated and untreated samples were clearly separated from each other and clustered according to their division (figure 16).

In addition, we presented another evidence of efficacy of treatment. We observed the upregulation of interferon, alpha-inducible protein 6 (IFI6) (19.4-fold; SD±4.6) and actin binding LIM protein family member 3 (ABLIM3) (19.3-fold; SD±3.8) in PCa cell lines in response to DNMT inhibitor zebularine (figure 15; tables 11 and 12). Both genes contain likely CpG island targets for methylation (figure 14) [39, 40, 49]. Furthermore,

Karpf et al. [84] reported that expression of the IFN-induced gene set is not due to nonspecific cellular toxicity or growth arrest after treatment of HT29 colon adenocarcinoma cells with 5-Aza-CdR, but that it is regulated by hypermethylation of its promoter. Consequently, we assume that at least IFI6 was directly silenced by de novo methylation in tumor cell lines and expressed after being exposed with zebularine.

4.2 Computational analyses

Particular emphasis was given to rational selection of candidate genes. First, we performed three biological replication microarray analyses for both treated and control cells in both lines in order to understand and control the sources of noise in the process and to eliminate them [85]. These helped us to identify particular genes with the desired number of replicates. Next, we categorized them according to the "fold-change" expression, after exposing PCa cell lines to zebularine. Pooling data from replicates allowed us to make a more reliable analysis of gene expression data. The number of probe sets that shared ≥1.5-fold upregulation was 85 in DU-145 and 31 in LNCaP (figure 17). The meaningful expression level was set to 2-fold [86]. 68 transcripts in DU-145 and 24 transcripts in LNCaP were 2-fold upregulated. Although the estimation of the extent of fold change is not very precise due to the different binding affinities to capture probes, microarray is still the method of choice for gene expression comparison. Finally, microarray results were validated by RT-qPCR (figure 15; tables 11 and 12), computational analyses (figure 16) and sources from literature (see chapter 4.1) [87].

The detection of one or multiple CpG islands in the promoter region of a particular gene is thought to be a strong indicator for methylation-dependent gene regulation [39, 40, 49] and was considered as the second criterion for candidate selection. Indeed, in 63 of 91 (69.2%) genes, CpG island(s) were detected. Expressed genes with no canonical CpG islands may also contain mC residues in their promoter, but to a lesser density that may not necessarily exclude a methylation/demethylation-based gene regulation. Besides, for a subset of genes, other means of upregulation (e. g. activation of cellular stress response) may be considered during the zebularine treatment [82].

Serial Analysis of Gene Expression (SAGE) was applied as the third candidate selection criterion. From a theoretical point of view, suitable candidates should show at least the same or higher expression level in normal tissue when compared to tumor

tissue (figure 10). In our case 60.4% (55/91) of genes were equally regulated and 21% (19/91) of genes were downregulated in tumor tissue. At the end, we generated a list of 51 candidate genes that were at least 2-fold upregulated, contain CpG islands and that were equally or overexpressed in normal tissue compared with tumor tissue (Digital Northern). The median “fold change” of our 51 selected candidates is 2.51 (2.01-4.52) (table 13).

4.3 RT-qPCR with special emphasis on reference gene selection

The selection of suitable reference genes for RT-qPCR is crucial, since it may dramatically influence the RGE value and can have major effects on the profiling result. In this context the reference gene should exhibit a similar expression level among the investigated groups and should not be regulated [73]. HPRT1 is proposed as a candidate reference gene by many groups working in the PCa field [72, 74, 88]. In particular Ohl et al. [72] recommended the single use of HPRT1, ALAS1, and K-ALPHA-1 or a combination of HPRT1/ALAS1 for target gene expression normalization. The authors found that the commonly used PBGD was not suitable for PCa mRNA profiling [72].

Since, we found that all common reference genes (HPRT1, TBP, and PBGD) were regulated in our experiments (figure 18), advanced models and algorithm-based software for reference gene selection was applied. GeNorm^{PLUS} calculated that the chosen genes display a high expression stability, with M values ranging from 0.85 (TBP) to 0.59 (PBGD) (figure 19). However, geNorm^{PLUS} did not recommend any combination of reference genes due to higher VNF values than the suggested cutoff value (cut-off value for proper normalization is less than 0.15, see chapter 3.10). Finally, we used PBGD with the lowest M value for RGE normalization of our candidate genes. In summary, for optimal results, reference genes have to be selected individually for each experimental approach [89].

4.4 Candidate genes

In this study, we report on the mRNA expression of the selected candidate genes POTEF, ABLIM3, IFI6, CTH, ASNS, SPRY4, GADD45A, and SARS in a set of 50 matched pairs of human prostate normal and tumor tissue.

POTEF was the only gene among the candidates that displayed a significantly increased expression ($P<0.001$) in the majority of tumor samples. Statistical analysis of mRNA expression of two other genes, CTH ($P=0.48$), and IFI6 ($P=0.28$), did not show

any statistically meaningful differences between adjacent normal and tumor prostate tissue samples (figure 20). ABLIM3 (P=0.063) demonstrated only a trend for downregulation in tumor samples. The expression patterns of these genes did not correspond to our experimental hypothesis and were therefore excluded from further investigation.

We focused on significantly downregulated genes in PCa in accordance with our working hypothesis. We comprehensively examined the mRNA expression of four candidate transcripts, namely ASNS, SPRY4, GADD45A, and SARS as well as GSTP1 as the presumed "gold standard" for methylation-regulated genes in PCa. The results were statistically evaluated, specificity and sensitivity assessed. The functional importance of these four candidates for PCa biology will be discussed below.

4.4.1 SPRY4 and GADD45A

In agreement with the purpose of our experimental work, some of the genes downregulated in our study were already known to be hypermethylated in PCa. Sprouty homolog 4 (SPRY4) is located on chromosome 5q31.3. It participates in inhibiting of the growth factor-induced cell responses by inhibiting the RTK-dependent Ras/MAP (mitogen-activated protein) kinase signaling pathway [90, 91]. In this way members of the SPRY family are involved in the inhibition of various growth factors, such as: epidermal growth factor (EGF) receptor, fibroblast growth factor (FGF) receptor, vascular endothelial growth factor receptor (VEGF), and platelet-derived growth factor receptor (PDGF-R) [91, 92].

SPRY4 was found to be inactivated in non-small cell lung cancer (NSCLC) and dysplastic cell lines. Its re-expression in NSCLC cells increased cell differentiation and led to decreasing proliferation of transformed cells, as well as migration and invasion [92]. The most important finding in the context of our work is that SPRY4 is indeed repressed due to promoter and 5‘-flanking CpG island hypermethylation in a LNCaP cell line and tissue samples as reported by Wang et al. [76]. Moreover these authors could show that the repression of SPRY4 correlated with the methylation status of cytosine nucleotides as revealed by bisulphite sequencing [76]. After treatment of PCa cell lines with the DNMT inhibitor 5 Aza-CdR, SPRY4 was restored only in androgen-sensitive LNCaP cells. In addition, Wang et al. [76] observed that overexpression of transfected pcDNA-Sproty4 did not inhibit cell proliferation, but may increase cell migration. In our experiments SPRY4 exhibited a significant downregulation (P<0.0007; 44/50; 88%) in

the majority of tumor specimens and 31 of 37 samples (84%) were ≥-1.5-fold (median = -1.64) downregulated (figure 21; table 14). These results and the observation that a close relative, SPRY2, is also regulated by epigenetic modification provide further evidence of the important role members of the SPRY family play as putative tumor suppressors in PCa [93]. However, it remains to be shown, whether downregulation of its mRNA expression translates to the respective protein levels.

Growth arrest and DNA-damage-inducible alpha (GADD45A; DDIT1) and the other members of the GADD45 family are involved in the regulation of the cell cycle, DNA repair, apoptosis and inhibition of cell growth. GADD45A responds to ambient stress by activating of the stress induced p38/c-jun NH_2 terminal kinase pathway, finally leading to apoptosis and senescence [94]. Moreover, GADD45A suppresses tumor angiogenesis by blocking the mTOR/STAT3 pathway [95].

Tront et al. [96] reported that GADD45A may act in two ways in breast cancer, depending on the nature of the oncogenic trigger. First, it functions as a tumor suppressor in Ras-driven breast tumorigenesis via increasing JNK-mediated apoptosis and p38-mediated senescence. Second, GADD45A promotes Myc-driven breast cancer by negatively regulating MMP10 via GSK3 b/b-catenin signaling, resulting in increased tumor vascularization and growth [96]. Moreover, it was found to be hypermethylated in breast cancer, gastric cardia adenocarcinoma and acute myeloid leukemia [97-99].

In addition, GADD45A was reported by Ramachandra et al. [77] to be suppressed due to hypermethylation in PCa cell lines and primary tumors. The authors also proposed its suitability as a potential therapeutic target. The group revealed an inverse correlation between methylation of 5’ 4 CpG sites at the proximal promoter and gene expression. Also, Ramachandra et al. [77] observed that 5-Aza-CdR induces expression of GADD45A enhanced docetaxel sensibility in DU-145 and LNCaP cells. In our experiments, GADD45A exhibited significant downregulation ($P<0.0001$; 44/50; 84%) in the majority of tumor specimens and 37 of 44 (84%) were ≥-1.5-fold downregulated (figure 21; table 14). Our results and observations support the fact that GADD45A acts as a tumor suppressor and may be a suitable target for treatment of PCa.

Our results are supported by correlation analyses and ROC analyses, too. The Spearman correlation coefficients showed a strong positive correlation between SPRY4, GADD45A and GSTP1 (table 16). This correlation may be explained by the fact that all these 3 genes were found hypermethylated in PCa [49, 76, 77]. In addition GADD45A

and SPRY4 suppress tumor angiogenesis by suppressing VEGFA and VEGF [92, 95]. Inhibition of cell proliferation is another mechanism by which GADD45A and SPRY4 are functionally connected [90, 91, 94]. However, putative diagnostic properties of mRNA expression of these candidate genes at the given sensitivity cutoff of 90% indicate the acceptable specificities only for GSTP1 (78%) and GADD45A (58%), but not for SPRY4 (16%). Calculated AUCs were 0.841, 0.884 and 0.644 in GADD45A, GSTP1 and SPRY4, respectively (figure 22; table 15).

4.4.2 ASNS

The third repressed candidate gene in PCa is asparagine synthetase (ASNS; TS11), located on chromosome 7q21.3 and involved in the synthesis of asparagine by conversion of aspartate and glutamine to asparagine and glutamate [100].

There is evidence that this gene was silenced due to promoter methylation in bone marrow samples, Jensen rat sarcoma cells and human leukemic cell lines. Also, there is evidence that human ASNS activity is highly regulated in response to cell stress [100]. An example of this are the genomic elements and stress in endoplasmic reticulum that control ASNS transcription through the C/EBP-ATF response element (CARE) within the promoter and the PERK-eIF2-ATF4 arm of the unfolded protein response (UPR), respectively [100].

There are some controversial issues with regard to ASNS function in PCa biology. Sircar et al. [101] reported that ASNS is expressed in castration-resistant PCa. Although we did not examine castration-resistant PCa tissue in our study, ASNS was certainly downregulated (RGE) in 37 of 50 tumor tissues (74%; P=0.0007). However, only 44% of the downregulated samples (16/36) displayed a ≥-1.5-fold change in expression (figure 21; table 14). Using a comparable epigenetical work flow, Ibragimova et al. [82] reported ASNS upregulation by inhibitors 5Aza-dC and trichostatin A, and it was found to be unmethylated in PCa cell lines. In general, we cannot exclude the possibility that ASNS behaves differently in tissue and in cell lines.

4.4.3 SARS

The most surprising finding of our study was the behavior of gene SARS (seryl-tRNA synthetase), also known as SERS or SERRS. It is located on chromosome 1p13.3 and belongs to the class II aminoacyl tRNA family [102]. SARS expression was significantly diminished in 42 prostate tumor tissues (84%, P<0.0001) when compared to matched adjacent normal tissues. In addition, more than half of the downregulated

samples displayed a ≥-1.5-fold change in expression (figure 21; table 14). We are not aware of any published data that describe a significant downregulation of SARS as observed in our study.

There is evidence that some aminoacyl-tRNA synthetases are involved in cancer progression [103], however, as already mentioned above, there is no information available on the function of SARS in PCa. The major function of seryl-tRNA synthetase is its involvement in catalyzing the ligation of serine to its cognate tRNA [102].

SARS contribution to carcinogenesis was further demonstrated by recognition of the c-Jun NH2 terminal peptide in apoptotic neuroblastoma cells with the c-Jun/cs45 antibody for cytoplasmic immunostaining [104]. Besides, SARS was also found to play a key role in selenium metabolism. Selenium itself contributes to many different functions inside cells, like antioxidant protection, enhanced carcinogen detoxification and immune surveillance, modulation of cell cycle and apoptosis, inhibition of tumor cell invasion, and inhibition of angiogenesis [105]. Several studies tried to link the selenium metabolism more directly to prostate carcinogenesis [106-108]. However, a proposed food supplementation with selenium appeared to have no effect on the PCa incidence [109].

Currently, studies on SARS focus on its function in vascular development. In particular SARS's UNE-S domain was linked to vascular endothelial growth factor A (VEGFA) expression [110, 111]. VEGFA is a major regulator of angiogenesis and vasculogenesis by binding and activation of two tyrosine kinase receptors, vascular endothelial growth factor receptor 1, Flt-1 (VEGFR1) and vascular endothelial growth factor receptor 2, KDR/Flk-1(VEGFR2) [112]. VEGFR-1 and VEGFR-2 are indeed expressed in PCa, prostatic intraepithelial neoplasia, and basal cells of normal glands [113, 114]. Our group recently aimed to link angiogenesis-related factors more closely to PCa progression by discovering decreased transcript levels of VEGFR2. Steiner and colleagues [115] found a significant repression of VEGFR2 and other endothelial factors such as CD34, CD146 and CAV1 in PCa tissue specimens. However, nothing is known about a possible interaction of SARS and its role in regulation of other endothelial cell factors.

SARS expression is strongly correlated with the expression of GADD45A and GSTP1 that are already known to be hypermethylated in PCa (table 16) [49, 77]. Moreover, we found that GADD45A and SARS are located on the same chromosome (table 17). However, to support this observation (e.g. mutual expression regulation),

additional in vitro analyses are indispensable. Using ROC curve analyses, we demonstrated a moderate specificity of 48% at a sensitivity cutoff of 90% for SARS. The P value <0.0001 and an AUC of 0.816 suggest that SARS RGE improves the prediction of PCa. The other two genes gave similar results in our ROC analyses. Both genes had comparable AUCs (GADD45A, AUC=0.841; GSTP1, AUC=0.884) (figure 22; table 15). However, we did not find any correlations with pathological parameters.

In conclusion, we demonstrate the potential suitability of GSTP1 and GADD45A to differentiate benign from malignant prostatic tissue. Moreover, our results strongly suggest hypermethylation of the SARS gene to be involved in its epigenetic downregulation in prostate cancer.

5 Conclusion

For many years, DNA methylation has attracted attention in basic cancer research by promising new putative cancer markers for diagnosis, prognosis and prediction of therapy outcome in PCa. Many genes with promoter hypermethylation have been already well documented in PCa. This thesis presents an epigenetic screen aimed to discover hitherto unknown genes that are downregulated by promoter hypermethylation in prostate cancer.

One way to identify epigenetically silenced genes in tumor cells is accomplished by using methylation inhibitors such as zebularine. We present experimental evidence that by using the DNMT inhibitor zebularine at an optimal concentration it is possible to effectively demethylate and thus reactivate certain genes in the PCa cell lines LNCaP and DU-145. Consequently, RNA from these treated cells was used to identify the respective upregulated transcripts. Additional criteria, such as presence of CpG islands and Digital Northern, were used for a rational candidate gene selection to confirm methylation-related events. The expression profiles for nine candidate genes were measured in 50 patients using paired samples of adjacent normal and tumor prostate tissue by RT-qPCR.

SARS, GADD45A, SPRY4, ASNS, and GSTP1 were significantly downregulated in tumor samples when compared to adjacent normal samples. The diagnostic potential was calculated by receiver operating characteristic curves. SARS (AUC=0.816) have a comparable AUC with regard to value and shape with GADD45A (AUC=0.841) and GSTP1 (AUC=0.884). Also, positive Spearman correlations were found between the relative gene expression levels of SARS, GADD45A and GSTP1. The presented data also suggest that GSTP1 and GADD45A may constitute potential tissue based biomarkers for prostate cancer detection. Moreover, we show for the first time that mRNA expression levels of SARS are decreased in PCa tissue compared to adjacent benign samples. According to our findings downregulation of SARS in PCa is most probably due to epigenetic downregulation by promoter hypermethylation and may encourage further studies on the potential role of SARS during the development, progression and even treatment of prostate cancer.

References

[1] Ferlay, J., Soerjomataram, I., Ervik, M., Dikshit, R., Eser, S., Mathers, C., Rebelo, M., Parkin, D., M. , Forman, D., and Bray, F., 2013, "GLOBOCAN 2012 v1.0,," Cancer Incidence and Mortality Worldwide: IARC CancerBase No. 11 [Internet]. International Agency for Research on Cancer, Lyon, France.
[2] Martin, D., Anne, S.-R., and Jutta, E., 2013, "Epidemiology of Prostate Cancer," Advances in Prostate Cancer, H. Gerhard, ed., InTech, Rijeka, Croatia, pp. 3-17.
[3] Baras, N., Barnes, B., Bertz, J., Dahm, S., Haberland, J. r., Kraywinkel, K., Laudi, A., and Wolf, U., 2012, "Krebs in Deutschland 2007/2008," R. Koch-Institut, ed., Gesellschaft der epidemiologischen Krebsregister in Deutschland e.V., Berlin, Deutschland.
[4] Hemminki, K., 2012, "Familial risk and familial survival in prostate cancer," World journal of urology, 30(2), pp. 143-148.
[5] Kheirandish, P., and Chinegwundoh, F., 2011, "Ethnic differences in prostate cancer," British journal of cancer, 105(4), pp. 481-485.
[6] Gustavo, F. C., Deborah, S. S., Douglas, E. M., Christian, R., and William, J. C., 1999, "Digital rectal examination for detecting prostate cancer at prostate specific antigen levels of 4 ng/ml or less " J Urol, 161, pp. 835-839.
[7] McNeal, J. E., Redwine, E. A., Freiha, F. S., and Stamey, T. A., 1988, "Zonal distribution of prostatic adenocarcinoma. Correlation with histologic pattern and direction of spread.," Am J Surg Pathol, 12(12), pp. 897-906.
[8] Stamey, T. A., Yang, N., Hay, A. R., McNeal, J. E., Freiha, F. S., and Redwine, E., 1987, "Prostate-Specific Antigen as a Serum Marker for Adenocarcinoma of the Prostate," N Engl J of Med, 317(15), pp. 909-916.
[9] Stephan, C., Vincendeau, S., Houlgatte, A., Cammann, H., Jung, K., and Semjonow, A., 2013, "Multicenter evaluation of [-2]proprostate-specific antigen and the prostate health index for detecting prostate cancer," Clinical chemistry, 59(1), pp. 306-314.
[10] Catalona, W. J., Richie, J. P., Ahmann, F. R., Hudson, M. A., Scardino, P. T., Flanigan, R. C., deKernion, J. B., Ratliff, T. L., Kavoussi, L. R., and Dalkin, B. L., 1994, "Comparison of digital rectal examination and serum prostate specific antigen in the early detection of prostate cancer: results of a multicenter clinical trial of 6,630 men.," J Urol, 151(5), pp. 1283-1290.
[11] Jung, K., Stephan, C., Lein, M., Henke, W., Schnorr, D., Brux, B., Schurenkamper, P., and Loening, S. A., 1996, "Analytical performance and clinical validity of two free prostate-specific antigen assays compared," Clinical chemistry, 42(7), pp. 1026-1033.
[12] Stephan, C., Jung, K., Semjonow, A., Schulze-Forster, K., Cammann, H., Hu, X., Meyer, H. A., Bogemann, M., Miller, K., and Friedersdorff, F., 2013, "Comparative assessment of urinary prostate cancer antigen 3 and TMPRSS2:ERG gene fusion with the serum [-2]proprostate-specific antigen-based prostate health index for detection of prostate cancer," Clinical chemistry, 59(1), pp. 280-288.
[13] Stephan, C., Cammann, H., Meyer, H. A., Muller, C., Deger, S., Lein, M., and Jung, K., 2008, "An artificial neural network for five different assay systems of prostate-specific antigen in prostate cancer diagnostics," BJU international, 102(7), pp. 799-805.
[14] Hessels, D., Klein, G., Jacqueline, M. T., Inge, v. O., Karthaus, H. F. M., Geert, J. L. v. L., Bianca, v. B., Kiemeney, L. A., Witjes, J. A., and Schalken, J. A., 2003, "DD3PCA3-based Molecular Urine Analysis for the Diagnosis of Prostate Cancer," Eur Urol, 44(1), pp. 8-16.
[15] Deras, I. L., Aubin, S. M., Blase, A., Day, J. R., Koo, S., Partin, A. W., Ellis, W. J., Marks, L. S., Fradet, Y., Rittenhouse, H., and Groskopf, J., 2008, "PCA3: a molecular urine assay for predicting prostate biopsy outcome," J Urol, 179(4), pp. 1587-1592.
[16] Sokoll, L. J., Wang, Y., Feng, Z., Kagan, J., Partin, A. W., Sanda, M. G., Thompson, I. M., and Chan, D. W., 2008, "[-2]proenzyme prostate specific antigen for prostate cancer detection: a national cancer institute early detection research network validation study," J Urol, 180(2), pp. 539-543.
[17] Demichelis, F., Fall, K., Perner, S., Andren, O., Schmidt, F., Setlur, S. R., Hoshida, Y., Mosquera, J. M., Pawitan, Y., Lee, C., Adami, H. O., Mucci, L. A., Kantoff, P. W., Andersson, S. O., Chinnaiyan, A. M., Johansson, J. E., and Rubin, M. A., 2007, "TMPRSS2:ERG gene fusion

associated with lethal prostate cancer in a watchful waiting cohort," Oncogene, 26(31), pp. 4596-4599.
[18] Jonathan, I. E., William, C. A., Mahul, B. A., and Lars, L. E., 2005, "The 2005 International Society of Urological Pathology (ISUP) Consensus Conference on Gleason Grading of Prostatic Carcinoma," J Surg Pathol, 29(9), pp. 1228-1242.
[19] Adolfsson, J., Tribukait, B., and Levitt, S., 2007, "The 20-Yr outcome in patients with well- or moderately differentiated clinically localized prostate cancer diagnosed in the pre-PSA era: the prognostic value of tumour ploidy and comorbidity," Eur Urol, 52(4), pp. 1028-1035.
[20] Jonsson, E., Sigbjarnarson, H. P., Tomasson, J., Benediktsdottir, K. R., Tryggvadottir, L., Hrafnkelsson, J., Olafsdottir, E. J., Tulinius, H., and Jonasson, J. G., 2006, "Adenocarcinoma of the prostate in Iceland: a population-based study of stage, Gleason grade, treatment and long-term survival in males diagnosed between 1983 and 1987," Scandinavian journal of urology and nephrology, 40(4), pp. 265-271.
[21] Adolfsson, J., 2008, "Watchful waiting and active surveillance: the current position," BJU international, 102(1), pp. 10-14.
[22] Klotz, L., 2005, "Active surveillance with selective delayed intervention is the way to manage 'good-risk' prostate cancer," Nature clinical practice. Urology, 2(3), pp. 136-142.
[23] Bianco, F. J., Jr., Scardino, P. T., and Eastham, J. A., 2005, "Radical prostatectomy: long-term cancer control and recovery of sexual and urinary function ("trifecta")," Urology, 66(5 Suppl), pp. 83-94.
[24] Droz, J. P., Balducci, L., Bolla, M., Emberton, M., Fitzpatrick, J. M., Joniau, S., Kattan, M. W., Monfardini, S., Moul, J. W., Naeim, A., van Poppel, H., Saad, F., and Sternberg, C. N., 2010, "Background for the proposal of SIOG guidelines for the management of prostate cancer in senior adults," Critical reviews in oncology/hematology, 73(1), pp. 68-91.
[25] Bolla, M., Van Tienhoven, G., Warde, P., Dubois, J. B., Mirimanoff, R. O., Storme, G., Bernier, J., Kuten, A., Sternberg, C., Billiet, I., Torecilla, J. L., Pfeffer, R., Cutajar, C. L., Van der Kwast, T., and Collette, L., 2010, "External irradiation with or without long-term androgen suppression for prostate cancer with high metastatic risk: 10-year results of an EORTC randomised study," The lancet oncology, 11(11), pp. 1066-1073.
[26] Bolla, M., Collette, L., Blank, L., Warde, P., Dubois, J. B., Mirimanoff, R. O., Storme, G., Bernier, J., Kuten, A., Sternberg, C., Mattelaer, J., Lopez Torecilla, J., Pfeffer, J. R., Lino Cutajar, C., Zurlo, A., and Pierart, M., 2002, "Long-term results with immediate androgen suppression and external irradiation in patients with locally advanced prostate cancer (an EORTC study): a phase III randomised trial," Lancet, 360(9327), pp. 103-106.
[27] Hanahan, D., and Weinberg, R. A., 2011, "Hallmarks of cancer: the next generation," Cell, 144(5), pp. 646-674.
[28] Futreal, P. A., Coin, L., Marshall, M., Down, T., Hubbard, T., Wooster, R., Rahman, N., and Stratton, M. R., 2004, "A census of human cancer genes," Nature reviews. Cancer, 4(3), pp. 177-183.
[29] Herman, J. G., and Baylin, S. B., 2003, "Gene silencing in cancer in association with promoter hypermethylation," The New England journal of medicine, 349(21), pp. 2042-2054.
[30] Luo, J., Solimini, N. L., and Elledge, S. J., 2009, "Principles of cancer therapy: oncogene and non-oncogene addiction," Cell, 136(5), pp. 823-837.
[31] Taylor, B. S., Schultz, N., Hieronymus, H., Gopalan, A., Xiao, Y., Carver, B. S., Arora, V. K., Kaushik, P., Cerami, E., Reva, B., Antipin, Y., Mitsiades, N., Landers, T., Dolgalev, I., Major, J. E., Wilson, M., Socci, N. D., Lash, A. E., Heguy, A., Eastham, J. A., Scher, H. I., Reuter, V. E., Scardino, P. T., Sander, C., Sawyers, C. L., and Gerald, W. L., 2010, "Integrative genomic profiling of human prostate cancer," Cancer cell, 18(1), pp. 11-22.
[32] Marx, V., 2014, "Cancer genomes: discerning drivers from passengers," Nature Methods, 11(4), pp. 375-379.
[33] Lapointe, J., Li, C., Giacomini, C. P., Salari, K., Huang, S., Wang, P., Ferrari, M., Hernandez-Boussard, T., Brooks, J. D., and Pollack, J. R., 2007, "Genomic profiling reveals alternative genetic pathways of prostate tumorigenesis," Cancer research, 67(18), pp. 8504-8510.

[34] Gurel, B., Iwata, T., Koh, C. M., Jenkins, R. B., Lan, F., Van Dang, C., Hicks, J. L., Morgan, J., Cornish, T. C., Sutcliffe, S., Isaacs, W. B., Luo, J., and De Marzo, A. M., 2008, "Nuclear MYC protein overexpression is an early alteration in human prostate carcinogenesis," Modern pathology : an official journal of the United States and Canadian Academy of Pathology, Inc, 21(9), pp. 1156-1167.
[35] Lei, Q., Jiao, J., Xin, L., Chang, C. J., Wang, S., Gao, J., Gleave, M. E., Witte, O. N., Liu, X., and Wu, H., 2006, "NKX3.1 stabilizes p53, inhibits AKT activation, and blocks prostate cancer initiation caused by PTEN loss," Cancer cell, 9(5), pp. 367-378.
[36] Squire, J. A., 2009, "TMPRSS2-ERG and PTEN loss in prostate cancer," Nature genetics, 41(5), pp. 509-510.
[37] Abou-Kheir, W. G., Hynes, P. G., Martin, P. L., Pierce, R., and Kelly, K., 2010, "Characterizing the contribution of stem/progenitor cells to tumorigenesis in the Pten-/-TP53-/- prostate cancer model," Stem Cells, 28(12), pp. 2129-2140.
[38] Berger, S. L., Kouzarides, T., Shiekhattar, R., and Shilatifard, A., 2009, "An operational definition of epigenetics," Genes & development, 23(7), pp. 781-783.
[39] Perry, A. S., Watson, R. W., Lawler, M., and Hollywood, D., 2010, "The epigenome as a therapeutic target in prostate cancer," Nature reviews. Urology, 7(12), pp. 668-680.
[40] Dawson, M. A., and Kouzarides, T., 2012, "Cancer epigenetics: from mechanism to therapy," Cell, 150(1), pp. 12-27.
[41] Barski, A., Cuddapah, S., Cui, K., Roh, T. Y., Schones, D. E., Wang, Z., Wei, G., Chepelev, I., and Zhao, K., 2007, "High-resolution profiling of histone methylations in the human genome," Cell, 129(4), pp. 823-837.
[42] Ellinger, J., Kahl, P., von der Gathen, J., Rogenhofer, S., Heukamp, L. C., Gutgemann, I., Walter, B., Hofstadter, F., Buttner, R., Muller, S. C., Bastian, P. J., and von Ruecker, A., 2010, "Global levels of histone modifications predict prostate cancer recurrence," The Prostate, 70(1), pp. 61-69.
[43] Roth, S. Y., Denu, J. M., and Allis, C. D., 2001, "Histone acetyltransferases," Annual review of biochemistry, 70, pp. 81-120.
[44] Ambs, S., Prueitt, R. L., Yi, M., Hudson, R. S., Howe, T. M., Petrocca, F., Wallace, T. A., Liu, C. G., Volinia, S., Calin, G. A., Yfantis, H. G., Stephens, R. M., and Croce, C. M., 2008, "Genomic profiling of microRNA and messenger RNA reveals deregulated microRNA expression in prostate cancer," Cancer research, 68(15), pp. 6162-6170.
[45] Friedman, J. M., Liang, G., Liu, C. C., Wolff, E. M., Tsai, Y. C., Ye, W., Zhou, X., and Jones, P. A., 2009, "The putative tumor suppressor microRNA-101 modulates the cancer epigenome by repressing the polycomb group protein EZH2," Cancer research, 69(6), pp. 2623-2629.
[46] Kikuchi, J., Takashina, T., Kinoshita, I., Kikuchi, E., Shimizu, Y., Sakakibara-Konishi, J., Oizumi, S., Marquez, V. E., Nishimura, M., and Dosaka-Akita, H., 2012, "Epigenetic therapy with 3-deazaneplanocin A, an inhibitor of the histone methyltransferase EZH2, inhibits growth of non-small cell lung cancer cells," Lung Cancer, 78(2), pp. 138-143.
[47] Baylin, S. B., 2005, "DNA methylation and gene silencing in cancer," Nature clinical practice. Oncology, 2 Suppl 1, pp. 4-11.
[48] Baylin, S. B., and Jones, P. A., 2011, "A decade of exploring the cancer epigenome - biological and translational implications," Nature reviews. Cancer, 11(10), pp. 726-734.
[49] Heyn, H., and Esteller, M., 2012, "DNA methylation profiling in the clinic: applications and challenges," Nature reviews. Genetics, 13(10), pp. 679-692.
[50] Li, E., Bestor, T. H., and Jaenisch, R., 1992, "Targeted mutation of the DNA methyltransferase gene results in embryonic lethality," Cell, 69(6), pp. 915-926.
[51] Gronbaek, K., Hother, C., and Jones, P. A., 2007, "Epigenetic changes in cancer," APMIS : acta pathologica, microbiologica, et immunologica Scandinavica, 115(10), pp. 1039-1059.
[52] Wu, H., and Zhang, Y., 2011, "Mechanisms and functions of Tet protein-mediated 5-methylcytosine oxidation," Genes & development, 25(23), pp. 2436-2452.
[53] Wu, H., and Zhang, Y., 2014, "Reversing DNA methylation: mechanisms, genomics, and biological functions," Cell, 156(1-2), pp. 45-68.
[54] Gal-Yam, E. N., Saito, Y., Egger, G., and Jones, P. A., 2008, "Cancer epigenetics: modifications, screening, and therapy," Annual review of medicine, 59, pp. 267-280.

[55] Stirzaker, C., Taberlay, P. C., Statham, A. L., and Clark, S. J., 2014, "Mining cancer methylomes: prospects and challenges," Trends in genetics : TIG, 30(2), pp. 75-84.
[56] Cheng, J. C., Matsen, C. B., Gonzales, F. A., Ye, W., Greer, S., Marquez, V. E., Jones, P. A., and Selker, E. U., 2003, "Inhibition of DNA methylation and reactivation of silenced genes by zebularine," Journal of the National Cancer Institute, 95(5), pp. 399-409.
[57] Flotho, C., Claus, R., Batz, C., Schneider, M., Sandrock, I., Ihde, S., Plass, C., Niemeyer, C. M., and Lubbert, M., 2009, "The DNA methyltransferase inhibitors azacitidine, decitabine and zebularine exert differential effects on cancer gene expression in acute myeloid leukemia cells," Leukemia, 23(6), pp. 1019-1028.
[58] Lemaire, M., Chabot, G. G., Raynal, N. J., Momparler, L. F., Hurtubise, A., Bernstein, M. L., and Momparler, R. L., 2008, "Importance of dose-schedule of 5-aza-2'-deoxycytidine for epigenetic therapy of cancer," BMC cancer, 8, pp. 128-138.
[59] Neureiter, D., Zopf, S., Leu, T., Dietze, O., Hauser-Kronberger, C., Hahn, E. G., Herold, C., and Ocker, M., 2007, "Apoptosis, proliferation and differentiation patterns are influenced by Zebularine and SAHA in pancreatic cancer models," Scandinavian journal of gastroenterology, 42(1), pp. 103-116.
[60] Chiam, K., Centenera, M. M., Butler, L. M., Tilley, W. D., and Bianco-Miotto, T., 2011, "GSTP1 DNA methylation and expression status is indicative of 5-aza-2'-deoxycytidine efficacy in human prostate cancer cells," PloS one, 6(9), p. e25634.
[61] Yoon, H. Y., Kim, Y. W., Kang, H. W., Kim, W. T., Yun, S. J., Lee, S. C., Kim, W. J., and Kim, Y. J., 2012, "DNA methylation of GSTP1 in human prostate tissues: pyrosequencing analysis," Korean journal of urology, 53(3), pp. 200-205.
[62] Lee, W. H., Morton, R. A., Epstein, J. I., Brooks, J. D., Campbell, P. A., Bova, G. S., Hsieh, W. S., Isaacs, W. B., and Nelson, W. G., 1994, "Cytidine methylation of regulatory sequences near the pi-class glutathione S-transferase gene accompanies human prostatic carcinogenesis," Proceedings of the National Academy of Sciences of the United States of America, 91(24), pp. 11733-11737.
[63] Saxena, A., Dhillon, V. S., Shahid, M., Khalil, H. S., Rani, M., Prasad, D. T., Hedau, S., Hussain, A., Naqvi, R. A., Deo, S. V., Shukla, N. K., Das, B. C., and Husain, S. A., 2012, "GSTP1 methylation and polymorphism increase the risk of breast cancer and the effects of diet and lifestyle in breast cancer patients," Experimental and therapeutic medicine, 4(6), pp. 1097-1103.
[64] Tchou, J. C., Lin, X., Freije, D., Isaacs, W. B., Brooks, J. D., Rashid, A., De Marzo, A. M., Kanai, Y., Hirohashi, S., and Nelson, W. G., 2000, "GSTP1 CpG island DNA hypermethylation in hepatocellular carcinomas," Int J Oncol, 16(4), pp. 663-676.
[65] Schulz, W. A., Elo, J. P., Florl, A. R., Pennanen, S., Santourlidis, S., Engers, R., Buchardt, M., Seifert, H. H., and Visakorpi, T., 2002, "Genomewide DNA hypomethylation is associated with alterations on chromosome 8 in prostate carcinoma," Genes, chromosomes & cancer, 35(1), pp. 58-65.
[66] Wang, Q., Williamson, M., Bott, S., Brookman-Amissah, N., Freeman, A., Nariculam, J., Hubank, M. J., Ahmed, A., and Masters, J. R., 2007, "Hypomethylation of WNT5A, CRIP1 and S100P in prostate cancer," Oncogene, 26(45), pp. 6560-6565.
[67] Benjamini, Y., and Hochberg, Y., 1995, "Controlling the False Discovery Rate: a Practical and Powerful Approach to Multiple Testing," J R Statist Soc, 57(1), pp. 289-300.
[68] Irmgard, O., Gudrun, T., and Cornelia, G., 2009, LightCycler® Real-Time PCR Systems-Application Manual, Roche Diagnostics GmbH, Germany.
[69] Livak, K. J., and Schmittgen, T. D., 2001, "Analysis of relative gene expression data using real-time quantitative PCR and the 2(-Delta Delta C(T)) Method," Methods, 25(4), pp. 402-408.
[70] Pfaffl, M. W., 2001, "A new mathematical model for relative quantification in real-time RT-PCR," Nucleic acids research, 29(9), pp. 2002-2007.
[71] Boon, K., Osorio, E. C., Greenhut, S. F., Schaefer, C. F., Shoemaker, J., Polyak, K., Morin, P. J., Buetow, K. H., Strausberg, R. L., De Souza, S. J., and Riggins, G. J., 2002, "An anatomy of normal and malignant gene expression," Proceedings of the National Academy of Sciences of the United States of America, 99(17), pp. 11287-11292.

[72] Ohl, F., Jung, M., Xu, C., Stephan, C., Rabien, A., Burkhardt, M., Nitsche, A., Kristiansen, G., Loening, S. A., Radonic, A., and Jung, K., 2005, "Gene expression studies in prostate cancer tissue: which reference gene should be selected for normalization?," J Mol Med (Berl), 83(12), pp. 1014-1024.
[73] Hellemans, J., Mortier, G., De Paepe, A., Speleman, F., and Vandesompele, J., 2007, "qBase relative quantification framework and software for management and automated analysis of real-time quantitative PCR data," Genome biology, 8(2), p. R19.
[74] Vandesompele, J., De Preter, K., Pattyn, F., Poppe, B., Van Roy, N., De Paepe, A., and Speleman, F., 2002, "Accurate normalization of real-time quantitative RT-PCR data by geometric averaging of multiple internal control genes," Genome biology, 3(7), p. RESEARCH0034.
[75] Chen, J. S., Coustan-Smith, E., Suzuki, T., Neale, G. A., Mihara, K., Pui, C. H., and Campana, D., 2001, "Identification of novel markers for monitoring minimal residual disease in acute lymphoblastic leukemia," Blood, 97(7), pp. 2115-2120.
[76] Wang, J., Thompson, B., Ren, C., Ittmann, M., and Kwabi-Addo, B., 2006, "Sprouty4, a suppressor of tumor cell motility, is down regulated by DNA methylation in human prostate cancer," The Prostate, 66(6), pp. 613-624.
[77] Ramachandran, K., Gopisetty, G., Gordian, E., Navarro, L., Hader, C., Reis, I. M., Schulz, W. A., and Singal, R., 2009, "Methylation-mediated repression of GADD45alpha in prostate cancer and its role as a potential therapeutic target," Cancer research, 69(4), pp. 1527-1535.
[78] Stresemann, C., Brueckner, B., Musch, T., Stopper, H., and Lyko, F., 2006, "Functional diversity of DNA methyltransferase inhibitors in human cancer cell lines," Cancer research, 66(5), pp. 2794-2800.
[79] Pulukuri., S. M. K., and Jasti, S. R., 2005, "Activation of p53/p21Waf1/Cip1 pathway by 5-aza-2'-deoxycytidine inhibits cell proliferation, induces pro-apoptotic genes and mitogen-activated protein kinases in human prostate cancer cells," Int J Oncol, 26(4), pp. 863-871.
[80] Walton, T. J., Li, G., Seth, R., McArdle, S. E., Bishop, M. C., and Rees, R. C., 2008, "DNA demethylation and histone deacetylation inhibition co-operate to re-express estrogen receptor beta and induce apoptosis in prostate cancer cell-lines," The Prostate, 68(2), pp. 210-222.
[81] Hurtubise, A., and Momparler, R. L., 2004, "Evaluation of antineoplastic action of 5-aza-2'-deoxycytidine (Dacogen) and docetaxel (Taxotere) on human breast, lung and prostate carcinoma cell lines," Anti-cancer drugs, 15(2), pp. 161-167.
[82] Ibragimova, I., Ibanez de Caceres, I., Hoffman, A. M., Potapova, A., Dulaimi, E., Al-Saleem, T., Hudes, G. R., Ochs, M. F., and Cairns, P., 2010, "Global reactivation of epigenetically silenced genes in prostate cancer," Cancer Prev Res (Phila), 3(9), pp. 1084-1092.
[83] Yu, Y. P., Paranjpe, S., Nelson, J., Finkelstein, S., Ren, B., Kokkinakis, D., Michalopoulos, G., and Luo, J. H., 2005, "High throughput screening of methylation status of genes in prostate cancer using an oligonucleotide methylation array," Carcinogenesis, 26(2), pp. 471-479.
[84] Karpf, A. R., Peterson, P. W., Rawlins, J. T., Dalley, B. K., Yang, Q., Albertsen, H., and Jones, D. A., 1999, "Inhibition of DNA methyltransferase stimulates the expression of signal transducer and activator of transcription 1, 2, and 3 genes in colon tumor cells," Proceedings of the National Academy of Sciences of the United States of America, 96(24), pp. 14007-14012.
[85] Mei-Ling, T. L., Frank, C. K., Whitmorei, G. A., and Jeffrey, S., 2000, "Importance of replication in microarray gene expression studies: Statistical methods and evidence from repetitive cDNA hybridizations.," PNAS, 97(18), pp. 9834–9839.
[86] Tarca, A. L., Romero, R., and Draghici, S., 2006, "Analysis of microarray experiments of gene expression profiling," American journal of obstetrics and gynecology, 195(2), pp. 373-388.
[87] Jaluria, P., Konstantopoulos, K., Betenbaugh, M., and Shiloach, J., 2007, "A perspective on microarrays: current applications, pitfalls, and potential uses," Microbial cell factories, 6, p. 4.
[88] de Kok, J. B., Roelofs, R. W., Giesendorf, B. A., Pennings, J. L., Waas, E. T., Feuth, T., Swinkels, D. W., and Span, P. N., 2005, "Normalization of gene expression measurements in tumor tissues: comparison of 13 endogenous control genes," Laboratory investigation; a journal of technical methods and pathology, 85(1), pp. 154-159.

[89] Radonić, A., Thulke, S., Mackay, I. M., Landt, O., Siegert, W., and Nitsche, A., 2004, "Guideline to reference gene selection for quantitative real-time PCR," Biochemical and biophysical research communications, 313(4), pp. 856-862.
[90] Sasaki, A., Taketomi, T., Kato, R., Saeki, K., Nonami, A., Sasaki, M., Kuriyama, M., Saito, N., Shibuya, M., and Yoshimura, A., 2003, "Mammalian Sprouty4 Suppresses Ras-Independent ERK Activation by Binding to Raf1," Cell Cycle, 2(4), pp. 280-281.
[91] Cabrita, M. A., Jaggi, F., Widjaja, S. P., and Christofori, G., 2006, "A functional interaction between sprouty proteins and caveolin-1," The Journal of biological chemistry, 281(39), pp. 29201-29212.
[92] Tennis, M. A., Van Scoyk, M. M., Freeman, S. V., Vandervest, K. M., Nemenoff, R. A., and Winn, R. A., 2010, "Sprouty-4 inhibits transformed cell growth, migration and invasion, and epithelial-mesenchymal transition, and is regulated by Wnt7A through PPARgamma in non-small cell lung cancer," Molecular cancer research : MCR, 8(6), pp. 833-843.
[93] McKie, A. B., Douglas, D. A., Olijslagers, S., Graham, J., Omar, M. M., Heer, R., Gnanapragasam, V. J., Robson, C. N., and Leung, H. Y., 2005, "Epigenetic inactivation of the human sprouty2 (hSPRY2) homologue in prostate cancer," Oncogene, 24(13), pp. 2166-2174.
[94] Alexandra, C., Xiaojin, S., Jennifer, T., Barbara, H., and Dan, A. L., 2009, "Stress sensor Gadd45 genes as therapeutic targets in cancer," Cancer Therapy(7), pp. 268–276.
[95] Yang, F., Zhang, W., Li, D., and Zhan, Q., 2013, "Gadd45a suppresses tumor angiogenesis via inhibition of the mTOR/STAT3 protein pathway," The Journal of biological chemistry, 288(9), pp. 6552-6560.
[96] Tront, J. S., Huang, Y., Fornace, A. J., Jr., Hoffman, B., and Liebermann, D. A., 2010, "Gadd45a functions as a promoter or suppressor of breast cancer dependent on the oncogenic stress," Cancer research, 70(23), pp. 9671-9681.
[97] Perugini, M., Iarossi, D. G., Kok, C. H., Cummings, N., Diakiw, S. M., Brown, A. L., Danner, S., Bardy, P., Bik To, L., Wei, A. H., Lewis, I. D., and D'Andrea, R. J., 2012, "GADD45A methylation predicts poor overall survival in acute myeloid leukemia and is associated with IDH1/2 and DNMT3A mutations," Leukemia, pp. 1588-1592.
[98] Guo, W., Dong, Z., Guo, Y., Chen, Z., Kuang, G., and Yang, Z., 2013, "Methylation-mediated repression of GADD45A and GADD45G expression in gastric cardia adenocarcinoma," International journal of cancer. Journal international du cancer, pp. 2043-2053.
[99] Wang, W., Huper, G., Guo, Y., Murphy, S. K., Olson, J. A., Jr., and Marks, J. R., 2005, "Analysis of methylation-sensitive transcriptome identifies GADD45a as a frequently methylated gene in breast cancer," Oncogene, 24(16), pp. 2705-2714.
[100] Balasubramanian, M. N., Butterworth, E. A., and Kilberg, M. S., 2013, "Asparagine synthetase: regulation by cell stress and involvement in tumor biology," American journal of physiology. Endocrinology and metabolism, 304(8), pp. 789-799.
[101] Sircar, K., Huang, H., Hu, L., Cogdell, D., Dhillon, J., Tzelepi, V., Efstathiou, E., Koumakpayi, I. H., Saad, F., Luo, D., Bismar, T. A., Aparicio, A., Troncoso, P., Navone, N., and Zhang, W., 2012, "Integrative molecular profiling reveals asparagine synthetase is a target in castration-resistant prostate cancer," The American journal of pathology, 180(3), pp. 895-903.
[102] Guo, M., Yang, X. L., and Schimmel, P., 2010, "New functions of aminoacyl-tRNA synthetases beyond translation," Nature reviews. Molecular cell biology, 11(9), pp. 668-674.
[103] Park, S. G., Schimmel, P., and Kim, S., 2008, "Aminoacyl tRNA synthetases and their connections to disease," Proceedings of the National Academy of Sciences of the United States of America, 105(32), pp. 11043-11049.
[104] Celia, C., Joan, R., and Josep, E. E., 2001, "Antibodies against c-Jun N-terminal peptide cross-react with neo-epitopes emerging after caspase-mediated proteolysis during apoptosis," J Neurochem, 77(3), pp. 904-915.
[105] Zeng, H., and Combs, G. F., Jr., 2008, "Selenium as an anticancer nutrient: roles in cell proliferation and tumor cell invasion," The Journal of nutritional biochemistry, 19(1), pp. 1-7.
[106] Clark, L. C., Combs, G. F., Jr., Turnbull, B. W., Slate, E. H., Chalker, D. K., Chow, J., Davis, L. S., Glover, R. A., Graham, G. F., Gross, E. G., Krongrad, A., Lesher, J. L., Jr., Park, H. K., Sanders, B. B., Jr., Smith, C. L., and Taylor, J. R., 1996, "Effects of selenium

supplementation for cancer prevention in patients with carcinoma of the skin. A randomized controlled trial. Nutritional Prevention of Cancer Study Group," JAMA : the journal of the American Medical Association, 276(24), pp. 1957-1963.
[107] Pourmand, G., Salem, S., Moradi, K., Nikoobakht, M. R., Tajik, P., and Mehrsai, A., 2008, "Serum selenium level and prostate cancer: a case-control study," Nutrition and cancer, 60(2), pp. 171-176.
[108] Peters, U., and Takata, Y., 2008, "Selenium and the prevention of prostate and colorectal cancer," Molecular nutrition & food research, 52(11), pp. 1261-1272.
[109] Algotar, A. M., Stratton, M. S., Ahmann, F. R., Ranger-Moore, J., Nagle, R. B., Thompson, P. A., Slate, E., Hsu, C. H., Dalkin, B. L., Sindhwani, P., Holmes, M. A., Tuckey, J. A., Graham, D. L., Parnes, H. L., Clark, L. C., and Stratton, S. P., 2013, "Phase 3 clinical trial investigating the effect of selenium supplementation in men at high-risk for prostate cancer," The Prostate, 73(3), pp. 328-335.
[110] Xu, X., Shi, Y., Zhang, H. M., Swindell, E. C., Marshall, A. G., Guo, M., Kishi, S., and Yang, X. L., 2012, "Unique domain appended to vertebrate tRNA synthetase is essential for vascular development," Nature communications, 3, p. 681.
[111] Herzog, W., Muller, K., Huisken, J., and Stainier, D. Y., 2009, "Genetic evidence for a noncanonical function of seryl-tRNA synthetase in vascular development," Circulation research, 104(11), pp. 1260-1266.
[112] Shibuya, M., 2006, "Differential roles of vascular endothelial growth factor receptor-1 and receptor-2 in angiogenesis," Journal of biochemistry and molecular biology, 39(5), pp. 469-478.
[113] Ferrer, F. A., Miller, L. J., Lindquist, R., Kowalczyk, P., Laudone, V. P., Albertsen, P. C., and Kreutzer, D. L., 1999, "Expression of vascular endothelial growth factor receptors in human prostate cancer," Urology, 54(3), pp. 567-572.
[114] Michael, W. J., Jacqueline, M. B., and Wayne, D. T., 1997, "Vascular endothelial growth factor (VEGF) expression in prostate cancer and benign prostate hyperplasia," J Urol, 157, pp. 2323-2328.
[115] Steiner, I., Jung, K., Miller, K., Stephan, C., and Erbersdobler, A., 2012, "Expression of endothelial factors in prostate cancer: a possible role of caveolin-1 for tumour progression," Oncology reports, 27(2), pp. 389-395.

Appendix

Curriculum Vitae

"My CV will not be published in the electronic version of my work for privacy reasons."

List of publications

1. **Ikromov O.**, Al-Kamal I., Magheli A., Ratert N., Sendeski M., Miller K., Krause H., Kempkensteffen C. Functional epigenetic analysis of prostate carcinoma - a role for seryl-tRNA synthetase (SARS)? **Journals of Biomarkers.** 2014 March. Epub.

2. Al-Kamal I., **Ikromov O.**, Tölle A., Florian F. T., Magheli A., Miller K., Krause H., Kempkensteffen C. An epigenetic screen unmasks metallothioneins as putative contributors to renal cell carcinogenesis. **Urologia Internationalis.** 2014 March. Epub. The first authorship is shared.

3. Sendeski MM., Liu ZZ., Perlewitz A., Busch JF., **Ikromov O.**, Weikert S., Persson PB., Patzak A. Functional characterization of isolated, perfused outermedullary descending human vasa recta. **Acta Physiologica** (Oxf). 2013 May;208(1):50-6.

4. Al-Kamal I., **Ikromov O.**, Tölle A., Krause H. An epigenetic screen demasks metallothioneins as putative contributors to renal cell carcinogenesis. **Der Urologe.** 2013 January;52(1):106. *Abstract. 4. Symposium. Urologische Forschung der Deutschen Gesellschaft für Urologie. Berlin 2012, Germany.*

5. Jandrig, B., **Ikromov, O.**, Al-Kamal, I., Wendler, J.J., Schostak, M., Miller, K., Krause, H. The role of PBRM1 as tumor suppressor gene in renal cell carcinomas. **Der Urologe.** 2013 January;52(1):107. *Abstract. 4. Symposium. Urologische Forschung der Deutschen Gesellschaft für Urologie. Berlin 2012, Germany.*

6. **Ikromov O.**, Al-Kamal I., Magheli A., Kempkensteffen C., Miller K., Krause H. Pharmacological reactivation of epigenetically regulated genes in prostate cancer. **Der Urologe.** 2013 January;52(1):115. *Abstract. 4. Symposium. Urologische Forschung der Deutschen Gesellschaft für Urologie. Berlin 2012, Germany.*

7. **Ikromov O.**, Jandrig B., Al-Kamal I., Schostak M., Miller K., Krause H. The SWI/SNF nucleosome-remodeling gene PBRM1-another tumor suppressor gene in renal cell carcinomas? **European Urology Supplements.** February 2012;11;e306. *Abstract. 27th Annual EAU Congress. Paris, France.*

8. Alidjanov N., Boboev A., **Ikromov O.** Roket (sildenafil) comparative evaluation of efficacy and safety in patients with erectile dysfunction. *Abstract. Conference on Strategic issues for men's reproductive health and demographic processes in the Member States of the Eurasian Economic Community. Almaty 2010, Kazakhstan.*

9. Alidjanov N., Boboev A., **Ikromov O.** Treatment of abscess of prostate glands with transperineal access. *Abstract. Conference on Endourology and new technologies. Moscow 2010, Russia.*

10. **Ikromov O.** Feasibility of partial nephrectomy in patient with Renal Cell Carcinoma. ***Master thesis.*** *Tashkent Medical Academy. Tashkent 2008. Uzbekistan.*

Affidavit

“I, Odiljon, Ikromov certify under penalty of perjury by my own signature that I have submitted the thesis on the topic: “Pharmacological reactivation of epigenetically regulated genes for identification of therapeutic targets and putative biomarkers in prostate cancer.” I wrote this thesis independently and without assistance from third parties, I used no other aids than the listed sources and resources.

All points based literally or in spirit on publications or presentations of other authors are, as such, in proper citations (see "uniform requirements for manuscripts (URM)" the ICMJE www.icmje.org) indicated. The sections on methodology (in particular practical work, laboratory requirements, statistical processing) and results (in particular images, graphics and tables) correspond to the URM and are answered by me. My interests in any publications to this dissertation correspond to those that are specified in the following joint declaration with the responsible person and supervisor. All publications resulting from this thesis and which I am author correspond to the URM (see above) and I am solely responsible.

The importance of this affidavit and the criminal consequences of a false affidavit (section 156,161 of the Criminal Code) are known to me and I understand the rights and responsibilities stated therein.

Date Signature

Acknowledgements

First of all, I have to sincerely thank my supervisor Dr. Hans Krause for giving me the opportunity to join the urologic research group and conduct my doctoral thesis. He was a great teacher and always assisted me with planning and performing my work. Also, many thanks for my co-supervisor PD Dr. Carsten Kempkensteffen for advices to achieve this work and further cooperations.

I thank U. Ungethüm and the Charité LFGC core facility for processing data sets at their faculty. I greatly acknowledge the help of Waltraut Jekabsons to learn laboratory facilities, Hellmuth-Alexander Meyer to guiding me in bioinformatics and statistical analysis and Monika Jung to guiding me RT-qPCR technique and conducting all experiments. I also have to thank all other technicians and scientists, who always helped me in case of technical and scientific problems. Thanks to my friends Imad, Julia, Nadine and Zofia. I am very glad that met with you.

My work was supported by the European Association of Urology (EAU) Research fellowship and the Charité Promotionsstipendium. Many thanks for EAU Research fellowship and Charité Promotionsstipendium Boards.

Finally, thanks to my parents and to all other family members, for their unlimited and continuous encouragement, standing beside me and supporting in all my difficulties, believing in me and helping me to choose the right way to successful life.